

คอมพอสิตของเก้าแกลบ-อนุภาคแม่เหล็ก-พอลิไสตรีนเพื่อเป็นตัวดูดซับน้ำมัน

นางสาวณัฐธราภรณ์ วารีวิตร

วิทยานิพนธ์นี้เป็นส่วนหนึ่งของการศึกษาตามหลักสูตรปริญญาวิทยาศาสตรมหาบัณฑิต
สาขาวิชาปิโตรเคมีและวิทยาศาสตร์พอลิเมอร์
คณะวิทยาศาสตร์ จุฬาลงกรณ์มหาวิทยาลัย
ปีการศึกษา 2556
ลิขสิทธิ์ของจุฬาลงกรณ์มหาวิทยาลัย

บทคัดย่อและแฟ้มข้อมูลฉบับเต็มของวิทยานิพนธ์ตั้งแต่ปีการศึกษา 2554 ที่ให้บริการในคลังปัญญาจุฬาฯ (CUIR)
เป็นแฟ้มข้อมูลของนิสิตเจ้าของวิทยานิพนธ์ที่ส่งผ่านทางบัณฑิตวิทยาลัย

The abstract and full text of theses from the academic year 2011 in Chulalongkorn University Intellectual Repository (CUIR)
are the thesis authors' files submitted through the Graduate School.

COMPOSITES OF RICE HUSK ASH-MAGNETIC PARTICLE-POLYSTYRENE
AS OIL SORBENTS

Miss Natthaporn Warreewat

A Thesis Submitted in Partial Fulfillment of the Requirements
for the Degree of Master of Science Program in Petrochemistry and Polymer Science
Faculty of Science
Chulalongkorn University
Academic Year 2013
Copyright of Chulalongkorn University

Thesis Title	COMPOSITES OF RICE HUSK ASH-MAGNETIC PARTICLE-POLYSTYRENE AS OIL SORBENTS
By	Miss Natthaporn Warreewat
Field of Study	Petrochemistry and Polymer Science
Thesis Advisor	Assistant Professor Apichat Imyim, Ph.D.
Thesis Co-advisor	Numpon Insin, Ph.D.

Accepted by the Faculty of Science, Chulalongkorn University in Partial Fulfillment of the Requirements for the Master's Degree

..... Dean of the Faculty of Science
(Professor Supot Hannongbua, Dr. rer. nat.)

THESIS COMMITTEE

..... Chairman
(Assistant Professor Warinthorn Chavasiri, Ph.D.)

..... Thesis Advisor
(Assistant Professor Apichat Imyim, Ph.D.)

..... Thesis Co-advisor
(Numpon Insin, Ph.D.)

..... Examiner
(Associate Professor Wimonrat Trakarnpruk, Ph.D.)

..... External Examiner
(Panitan Wanakamol, Ph.D.)

ณัฐราภรณ์ วาริวัตร : คอมพอสิตของเถ้าแกลบ-อนุภาคแม่เหล็ก-พอลิสไตรีนเพื่อเป็นตัวดูดซับน้ำมัน. (COMPOSITES OF RICE HUSK ASH-MAGNETIC PARTICLE-POLYSTYRENE AS OIL SORBENTS) อ.ที่ปรึกษาวิทยานิพนธ์หลัก: ผศ.ดร.อภิชาติ อิมยิ้ม, อ.ที่ปรึกษาวิทยานิพนธ์ร่วม: ดร.นำพล อินสิน, 53 หน้า.

เถ้าแกลบมีซิลิกาเป็นองค์ประกอบสูงมากถึงร้อยละ 90 โดยน้ำหนักทำให้มีสมบัติในการดูดซับสารต่างๆ ได้เนื่องจากมีลักษณะที่มีความเป็นรูพรุนสูง ทำให้มีพื้นที่ผิวสูงงานวิจัยนี้ได้ทำการสังเคราะห์คอมพอสิตระหว่างเถ้าแกลบกับอนุภาคแม่เหล็กและนำมาเคลือบผิวด้วยพอลิสไตรีนเพื่อใช้เป็นวัสดุดูดซับน้ำมันจากน้ำโดยอนุภาคแม่เหล็กในวัสดุดูดซับทำให้สามารถแยกวัสดุดูดซับออกจากแหล่งปนเปื้อนด้วยแรงแม่เหล็กภายนอกได้การสังเคราะห์อนุภาคแม่เหล็กชนิดแมกนีไทต์ (Fe_2O_3) ใช้วิธีการตกตะกอนร่วมระหว่างเฟอร์ริกไอออน (Fe^{3+}) และเฟอร์รัสไอออน (Fe^{2+}) ในของผสมที่มีเถ้าแกลบ จากนั้นนำคอมพอสิตเถ้าแกลบ-อนุภาคแม่เหล็กไปเคลือบด้วยพอลิสไตรีนเพื่อทำให้พื้นผิวของวัสดุที่เตรียมได้มีสมบัติความไม่ชอบน้ำสูง ศึกษาตัวแปรที่มีผลต่อการดูดซับน้ำมันได้แก่ ปริมาณของอนุภาคแม่เหล็กและพอลิสไตรีนที่ผิวของเถ้าแกลบ และทำการพิสูจน์เอกลักษณ์ด้วยเทคนิคการเลี้ยวเบนรังสีเอกซ์เทคนิคกล้องจุลทรรศน์อิเล็กตรอนแบบส่องกราดและเอกซเรย์สเปกโทรสโกปีแบบกระจายพลังงาน เทคนิคฟูเรียร์ทรานสฟอร์มอินฟราเรดสเปกโทรสโกปี เทคนิคการเปลี่ยนแปลงน้ำหนักโดยอาศัยสมบัติทางความร้อนและหาปริมาณเหล็กในวัสดุดูดซับด้วยวิธีอะตอมมิคแอบซอร์พชันสเปกโทรเมตรีพบว่าเมื่อตกตะกอนร่วมอนุภาคแม่เหล็กบนพื้นผิวของเถ้าแกลบโดยใช้ปริมาณอนุภาคแม่เหล็กเริ่มต้นในอัตราส่วนร้อยละ 10-20 โดยน้ำหนักต่อน้ำหนักของเถ้าแกลบ จากนั้นนำมาแยกขนาดเป็นสองส่วนคือ 1-75 ไมครอน และ 75-150 ไมครอน พบว่าที่คอมพอสิตที่เตรียมจากปริมาณของอนุภาคแม่เหล็กเริ่มต้นร้อยละ 10 มีพื้นที่ผิวจำเพาะสูงสุดคือ 492 และ 545 ตารางเมตรต่อกรัมตามลำดับ และเมื่อนำคอมพอสิตมาเคลือบด้วยพอลิสไตรีนในอัตราส่วนร้อยละ 5-20 โดยน้ำหนักของพอลิสไตรีนต่อน้ำหนักของคอมพอสิตเถ้าแกลบ-อนุภาคแม่เหล็กพบว่าที่คอมพอสิตเถ้าแกลบ-อนุภาคแม่เหล็กที่มีพอลิสไตรีนร้อยละ 10 มีการดูดซับน้ำมันสูงสุดทั้งเท่ากับ 10.3 และ 12.5 กรัมต่อกรัมคอมพอสิต สำหรับเถ้าแกลบ-อนุภาคแม่เหล็กที่มีช่วงขนาด 1-75 ไมครอน และ 75-150 ไมครอนตามลำดับ

สาขาวิชาปิโตรเคมีและวิทยาศาสตร์พอลิเมอร์

ปีการศึกษา...2556.

ลายมือชื่อนิสิต.....

ลายมือชื่อ อ.ที่ปรึกษาวิทยานิพนธ์หลัก

ลายมือชื่อ อ.ที่ปรึกษาวิทยานิพนธ์ร่วม.....

5471963823 : MAJOR PETROCHEMISTRY AND POLYMER SCIENCE

KEYWORDS: RICE HUSK ASH / MAGNETIC PARTICLES / COMPOSITE / OIL SORBENT / POLYSTYRENE

NATTHAPORN WARREEWAT: COMPOSITES OF RICE HUSK ASH-MAGNETIC PARTICLE-POLYSTYRENE AS OIL SORBENTS. ADVISOR: ASST. PROF. APICHAAT IMYIM, Ph.D, CO-ADVISOR: NUMPON INSIN, Ph.D. 53 pp.

Rice husk ash (RHA), a material mainly composed of silica of more than 90 % by weight, was applied to study the sorption because it has high surface area due to its high porosity. In this study, sorbents were prepared by combining RHA and magnetic particles as composites and coated with polystyrene for oil adsorption. The sorbents could be separated from the contaminated sources using an external magnetic force due to the incorporation of magnetic particles. The composites were synthesized using co-precipitation of ferric iron (Fe^{3+}), ferrous iron (Fe^{2+}) to form Fe_2O_3 in presence of RHA. The RHA/ Fe_2O_3 composite was coated by polystyrene (PS) in order to increase their surface hydrophobicity. The important variables affecting the oil adsorption are the amount of magnetic particles and polystyrene on RHA surface. RHA/ Fe_3O_4 -PS composites were successfully prepared and characterized by X-ray diffraction (XRD), scanning electron microscope (SEM), X-ray analysis (EDX), Fourier transform infrared spectroscopy (FT-IR), thermogravimetric analysis (TGA) and atomic absorption spectrometry (AAS). After preparing the magnetic particles on RHA surfaces using various quantities of Fe_3O_4 particles ranging from 10-20 %weight of Fe_3O_4 to weight of RHA, the composites were divided into two classes of size, i.e. 1-75 and 75-150 μm . The results showed that the composites with 10% of starting magnetic particles had the highest specific surface area of 492 and 545 m^2/g for 1-75 and 75-150 μm composites, respectively. RHA/ Fe_3O_4 composites were then modified with waste polystyrene foam of various weight percent ranging from 5–20 %weight of polystyrene to weight of RHA/ Fe_3O_4 composites. The results showed that the composites with 10% polystyrene had the highest oil adsorption capacity of 10.3 and 12.5 g/g for 1-75 and 75-150 μm sorbents, respectively.

Field of Study : Petrochemistry and Polymer

Academic Year : 2013

Student's Signature

Advisor's Signature

Co-advisor's Signature

ACKNOWLEDGEMENTS

I am especially grateful to my advisor, Assistant Professor Dr. Apichat Imyim and my co-advisor, Dr. Numpon Insin for their valuable guidance, assistance, inspiration, and generous encouragement throughout this research. I would like to extend my appreciation to Assistant Professor Dr. Fuangfa Unob for her precious suggestions. I wish to thank my graduate committee members, Assistant Professor Dr. Warinthorn Chavasiri, Associate Professor Dr. Wimonrat Trakarnprukand Dr. Panitan Wanakamol for serving as the chairman and members of this thesis committee, respectively, for their valuable suggestions and comments. Furthermore, I could be filled with kindness, encouragement, lovely friendship. I would like to thank all of my friends in the laboratory, the members of Environmental Analysis Research Unit. I greatly appreciate their kind assistance, generosity and encouragement throughout the course of my research and I would like to thank the members for their help and friendship. Finally, I would like to express my deepest gratitude to my father and my mother for their love and personal supports at all times.

CONTENTS

	Page
THAI ABSTRACT	iv
ENGLISH ABSTRACT	v
ACKNOWLEDGEMENTS	vi
CONTENTS	vii
LIST OF TABLES.....	xix
LIST OF FIGURES.....	xix
LIST OF ABBREVIATIONS.....	xix
CHAPTER I INTRODUCTION	1
1.1 Statement of the problem.....	1
1.2 Objectives	2
1.3 Scopes of this thesis	2
CHAPTER II THEORY	3
2.1 Rice husk and rice husk ash.....	3
2.1.1 Characteristics of rice husk	3
2.1.2 Preliminary treatment of rice husk and silica production	4
2.1.3 Form of silica.....	5
2.1.3.1 Amorphous silica	5
2.1.3.2 Crystalline silica	5
2.2 Magnetic Materials.....	6
2.2.1 Magnetic Properties	6
2.2.1.1 Paramagnetism.....	6
2.2.1.2 Ferromagnetism.....	6
2.2.1.3 Ferrimagnetism.....	7
2.2.1.4 Antiferromagnetism.....	7
2.2.1.5 Superparamagnetism.....	7
2.2.2 Iron based magnetic particles.....	7

	Page
2.2.2.1 Maghemite (γ - Fe_2O_3).....	9
2.2.2.2 Magnetite (Fe_3O_4).....	9
2.3 Polystyrene	10
2.4 Crude oil.....	12 12
2.4.1 Toxicity of crude oil.....	13
2.4.1.1 Acute (immediate) health risks.....	13
2.4.1.2 Chronic (long-term) health risks.....	14 14
2.4.2 Contamination of oil.....	14
2.4.2.1 Oil contamination in air.....	14
2.4.2.2 Oil Contamination in land	14
2.4.2.3 Oil Contamination in water	14
2.4.3 Removal of crude oil and treatment of oil spill	15
2.4.3.1 Mechanical techniques	15
2.4.3.2 Bioremediation.....	15
2.4.3.3 Dispersants.....	15
2.4.3.4 Sorbents	15
2.5 Literature review	16
2.5.1 Treatment of oil spill using adsorption process.....	16
2.5.2 Preparation of rice husk ash and its chemical modification.....	17
2.5.3 Utilisation of rice husk and rice husk ash as sorbents.....	18
CHAPTER III EXPERIMENTAL	20
3.1 Instruments.....	20
3.2 Chemicals	21 21
3.2.1 Preparation methods of chemicals and reagents.....	21
3.2.1.1 Sodium hydroxide solutions	21
3.2.1.2 Nitric acid solutions.....	21
3.2.1.3 Hydrochloric acid solutions.....	21

	Page
3.3 Preparation of Rice husk ash	21
3.4 Preparation of RHA/Fe ₃ O ₄	22 22
3.5 Preparation of RHA/Fe ₃ O ₄ -PS composite	23
3.6 Characterization of the composites	23
3.6.1 X-ray fluorescence analysis (XRF)	23
3.6.2 CHNS/O analysis	23
3.6.3 Atomic absorption spectroscopy (AAS).....	23
3.6.4 X-ray diffraction (XRD)	23
3.6.5 Contact angle	24
3.6.6 Scanning Electron Microscopy (SEM).....	24
3.6.7 Nitrogen adsorption technique.....	24
3.6.8 Fourier transform infrared spectroscopy (FT-IR).....	24
3.6.9 Thermogravimetric analysis.....	24
3.7 Oil adsorption experiments	25
CHAPTER IV RESULTS AND DISCUSSION	26
4.1 Characterization of the materials	26
4.1.1 X-ray fluorescence (XRF).....	26 26
4.1.2 CHNS/O elemental analysis	26 26
4.1.3 X-ray diffraction (XRD).....	27
4.1.3.1 The effect of Fe ₃ O ₄ amount.....	30
4.1.4 Surface area analysis	31
4.1.5 Thermogravimetric analysis (TGA).....	34
4.1.6 Contact angles	36
4.1.7 Fourier transforms infrared spectroscopy	37
4.1.8 SEM micrographs and EDX diffractograms.....	38
4.2 Adsorption study.....	41 41
4.2.1 Effect of RHA size.....	41

	Page
4.2.2 Effect of Fe ₃ O ₄ loading	4242
4.2.3 Effect of polystyrene loading	4242
4.2.4 Effect of contact time	4343
4.3 Separation of the composites from water/oil mixture by a magnet	45
CHAPTER V CONCLUSION	47
5.1 Conclusion	47
5.2 Suggestion	47
REFERENCES	48
VITA	53

LIST OF TABLES

	Page
Table 2.1 Chemical composition of dry rice husk.....	3
Table 2.2 Ash and silica contents of various plants	4
Table 2.3 Decomposition rates of natural and synthetic materials [24]	1111
Table 3.1 List of analytical instruments	2020
Table 3.2 Chemicals and suppliers.....	2121
Table 4.1 Chemical composition of RHA by XRF analysis	2626
Table 4.2 Chemical composition of rice husk ash by elemental analysis	2727
Table 4.3 Amount of Fe ₃ O ₄ observed in the RHA/Fe ₃ O ₄ composites.....	3131
Table 4.4 Textural characteristics for the RHA and the RHA/Fe ₃ O ₄ composites	3434
Table 4.5 FTIR vibration and their assignments for RHA, polystyrene, Fe ₃ O ₄ particles..	37
Table 4.6 Adsorption capacity of RHA/Fe ₃ O ₄ -PS composites	4141
Table 4.7 The maximum adsorption capacity of the RHA/Fe ₃ O ₄ -PS compared to other modified silica for oil adsorption.....	44

LIST OF FIGURES

	Page
Figure 2.1 Structure of silica and its functional groups [15]	4
Figure 2.2 Porous carbon from rice husk [19].....	6
Figure 2.3 The two magnetic A and B of a spinel structure [20].....	8
Figure 2.4 Cation distributions in normal spinel and inverse spinel. A and B indicate A atom and B atom cations, respectively [21].....	8
Figure 2.5 Chemical structure of (a) The inverse spinel Fe_3O_4 bulk unit cell containing O (red), tetrahedral Fe(A) atoms (<i>light blue</i>) and octahedral Fe (B) atoms (yellow) [22].....	9
Figure 2.6 Chemical structure of polystyrene	10
Figure 2.7 Schematic showing the spreading of oil on apolystyrene surface.....	1111
Figure 3.1 Rice husk and prepared rice husk ash	2222
Figure 4.1 X-ray diffraction pattern of pure RHA compared.....	2828
Figure 4.2 X-ray diffraction pattern of Fe_3O_4	2929
Figure 4.3 X-ray diffraction pattern of RHA, Fe_3O_4 , RHA/ Fe_3O_4 composites.....	3030
Figure 4.4 Nitrogen adsorption desorption isotherms	32
Figure 4.5 Thermogravimetric weight loss curve of RHA/ Fe_3O_4 -PS composites	35
Figure 4.6 Photographs showing a water droplet on the surface	36
Figure 4.7 FTIR the spectra of composite.....	3838
Figure 4.8 The SEM micrographs and EDX elemental mapping of RHA/ Fe_3O_4	3939
Figure 4.9 The SEM micrographs and EDX elemental mapping of RHA/ Fe_3O_4 -PS	3939
Figure 4.10 EDX diffractograms of (a) RHA@600 °C (b) RHA/ Fe_3O_4 -PS	4040
Figure 4.11 Adsorption capacity of the composites.....	4141
Figure 4.12 Adsorption capacity of RHA/ Fe_3O_4 composites were prepared by using different amount of Fe_3O_4	4242
Figure 4.13 Adsorption capacity of RHA/ Fe_3O_4 -PS composites were prepared by using different amount of polystyrene.....	4343
Figure 4.14 Effect of adsorption time on oil adsorption of RHA/ Fe_3O_4 -PS.....	4444
Figure 4.15 The demonstration removed adsorbent out of the contaminated area ...	46

LIST OF ABBREVIATIONS

°C	Degree Celsius
mL	Mililiter
g	gram(s)
Min	Minute
h	Hour
XRF	X-ray Fluorescence
AAS	Atomic Absorption Spectroscopy
FTIR	Fourier Transform Infrared Spectroscopy
TGA	Thermogravimetric Analysis
XRD	X-ray Diffraction
SEM	Scanning Electron Microscope
EDX	Energy Dispersive X-ray Spectroscopy
ASTM	American Society of Testing and Materials
RHA	Rice husk ash
PS	Polystyrene

CHAPTER I INTRODUCTION

1.1 Statement of the problem

In recent years, regular occurrence of oil spill on water surface causes many critical ecological problems. The main reasons of oil pollution in the ocean and other waterways are the leaking out of oil and fuel from land-based sources, accidental spills from tankers or underwater pipelines, and oil from refineries [1]. The contaminant sources are usually crude oil, which is determined as a highly complex mixture of aliphatic hydrocarbons, alicyclic hydrocarbons and aromatic hydrocarbons, with low percentages of sulfur and trace amounts of nitrogen and oxygen compounds [2]. Originally, oil spill cleanup techniques such as chemical dispersants [3], bioremediation [4], and adsorbent materials [5].

Normally, attributes of adsorbent materials are very good buoyancy, high oil sorption capacity, hydrophobic characteristics, and biodegradability [6]. Many types of sorbents have been studied for the use in removing oil from water. There are three types of sorbents; inorganic sorbents such as organoclays [6], perlite [7] and silica from calcined rice husk ash [5]. Second type is synthetic sorbent such as polyethylene, polypropylene, polyvinyl chloride, polystyrene and polyurethane [8]. Third is organic sorbents such as banana stalk, butyl rubber and peat [9].

Rice husk, which is an agricultural wastefrom rice milling process, generates abundant waste up to 25 % by the wet weight. However, it can be turned into useful starting materials for several utilizations. Prepared by a thermo-chemical process, rice husk ash is composed of silica (more than 90 % by weight) and other impurities [10]. Silica (SiO_2) is one of the valuable multipurpose inorganic compounds. It initially exists in the amorphous form. When combusted in high temperature, it exists in crystalline amorphous forms. The burning of RH in air always leads to the formation of silica ash varying in colours ranging from grey to black depending on inorganic impurities as well as unburned carbon contents. An attempt to remove the unburned carbon by further burning in higher temperatures ($> 700\text{ }^\circ\text{C}$) leads to the crystallisation of amorphous silica to be cristobalited [11]. If the rich husk ash has high cristobalited content, it will be harder to crush rice husk ash structure, resulting in the high surface area [12]. Burning rice husks at temperature below 650°C produces amorphous forms of rice husk ashes. Combination of 650°C temperature and 60 minutes burning time seems to present the optimized solution resulting in non-crystallized RHA.

Applications of rice husk ash (RHA) are such as desiccants, catalysts, catalyst supports and adsorbents [13]. RHA adopts porous structure with high specific surface

area. Nevertheless, the silica surface has hydrophilic silanol group that affects oil sorption ability because oil is non-polar in nature. Therefore, modifying RHA with polystyrene foam can make hydrophobic surfaces. In addition magnetic particles are also materials of interest due to their magnetic properties. Major incorporation advantage of magnetic particles is that the composite sorbents can be separated from oily wastewater by using a magnetic field. The magnetic particles were synthesized by a co-precipitation method because of its simplicity, productivity and low cost in the production process. In this work, new RHA-magnetic particle sorbents coated with polystyrene are prepared and the efficiency for oil removal is evaluated.

1.2 Objectives

The objectives of this study are listed below.

- (1) To synthesize composites of rice husk ash-magnetic particles-polystyrene to use as an oil sorbent.
- (2) To study suitable parameters for preparation of poly-styrene and magnetic particles compositing with ash for the most oil effective adsorption.

1.3 Scopes of this thesis

The scope of this study about rice husk ash (RHA) was to study oil spill sorption. In this study, sorbents were prepared by combining RHA and magnetic particles as composites that are easy to dispose out of water surface by mean of magnetic separation. Composites of RHA and magnetic particles were synthesized using co-precipitation of Fe^{3+} , Fe^{2+} and RHA using various quantities of Fe_3O_4 particles ranging from 10-20 %w/w. RHA/ Fe_3O_4 composites was then modified with waste polystyrene foam of various weight percent ranging from 5-20 %w/w. The prepared RHA/ Fe_3O_4 -PS composites were characterized by X-ray diffraction (XRD), scanning electron microscope (SEM), Energy-dispersive X-ray (EDX), Fourier transform infrared spectroscopy (FT-IR) and thermogravimetric analysis (TGA). The amount of Fe_3O_4 in RHA/ Fe_3O_4 was determined by atomic absorption spectrometry (AAS) after acid digestion of the solid. In addition, oil absorbency was measured by ASTM F726 method.

CHAPTER II THEORY

Suitable supported adsorbent used in industries are based on these properties: high surface area, porosity, and low cost. Silica is one of the most widely used supported materials because it is inexpensive, structurally stable and has a wide variety of the pore sizes. Silica based materials are available with surface areas in the range of 400-1000 m²/g. All of properties could be also found in rice husk ash silica.

2.1 Rice husk and rice husk ash

Rice husk (RH), an agricultural waste product from the refining of rice, is the natural sheaths that form on rice grains. It is often used as fuel for electricity generation and boiler in the rice mills. It would be beneficial for the environment to recycle these waste to produce eco-material [12]. End uses of wastes depend on its structure, properties and chemical composition.

2.1.1 Characteristics of rice husk

The chemical composition of dry rice husk and rice husk ash contain an average composition in the Table 2.1 [1].

Table 2.1 Chemical composition of dry rice husk [1]

Composition	Amount present in RH (%)
α -cellulose	43.3
Lignin	22.0
D-xylose	17.52
L-arabinose	6.53
Methylglucuronic acid	3.27
D-galactose	2.35
Other organic	5.03

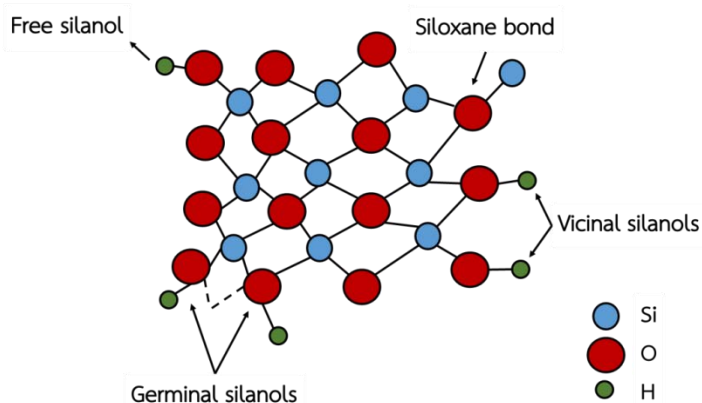
Of all the plant residues, The rice husk ash shows the highest amount of silicon contents when compare to other plants as shown in Table 2.2 [14]

Table 2.2 Ash and silica contents of various plants [14]

Plant	Part of plant	Ash (%)	Silica (%)
Rice	Grain sheath/husk	22.1	93.0
Wheat	Leaf sheath	10.5	90.5
Sorghum	Leaf sheath epidermis	12.5	88.7
Rice	Stem/straw	14.6	82.0
Breadfruit tree	Stem	8.6	81.8
Bagasse	-	14.7	73.0
Corn	Leaf blade	12.1	64.3
Bamboo	Nodes (inner portion)	1.5	57.4
Sunflower	Leaf and stem	11.5	25.3
Lantana	Leaf and stem	11.2	23.3

2.1.2 Preliminary treatment of rice husk and silica production

There are many methods for the extraction of silica from rich husk. Many researchers have suggested an acid preliminary treatment before thermal treatment for the extraction of silica. Preparatory leaching of the rice husk with a solution of HCl, HNO₃, H₂SO₄, NaOH, NH₄OH, boiled with temperature 500-1400 °C before thermal treatment to remove impurities and increase the purity of silica content. The acids like sulfuric, oxalic, and citric acids can be used for leaching of rice husk. However, examine silica of experimental results obtaining from hydrochloric acid has higher surface area than other acids [1]. The thermal treatment of rice husk ash does not affect the structure of ash-silica. Obtaining, high specific surface area of silica from the rice husk ash is possible. The functional groups on the surface of silica are classified to free silanol, vicinal silanol, germinal silanol as shown in Figure 2.1 [15].

**Figure 2.1** Structure of silica and its functional groups [15].

After thermal treatment, there are two major changes on rice husk ash, including volatile compound contents and husk structural characteristics. First change came from a release of volatile compounds during the thermal cracking of lignin-cellulose matrix, and the second is the change in hydrophobic/hydrophilic properties. These carbon residue and silanol surface are dispersed on the surface of solid pyrolysis residue and cause the ratio between these two components and will affect hydrophobicity. The hydrophobic carbon residues will boost the adsorption of petroleum hydrocarbons, while the hydrophilic silanol group helps the sorption of water [5].

2.1.3 Form of silica

Ash with high percentage of crystalline silica is formed during a burn of rice husk at high temperature. Nevertheless, if rice husk is burnt under controlled conditions (lower 500-600°C) it will produce highly reactive amorphous silica, that has different properties. It is used specifically to produce ash with high organic compound.

2.1.3.1 Amorphous silica

Amorphous silica is used as an industrial white mineral along with clay, CaCO₃, and talc. The amorphous forms of silica are composed of silica tetrahedral arranged in a random three-dimensional network without regular lattice structures. Amorphous silica has high purity, small particle size and high surface area. It can be used as an adsorbent or catalyst in chemical synthesis [16].

2.1.3.2 Crystalline silica

The crystalline forms of RHA are found at temperatures 800-1200 °C. Its crystallization has to be protected by controlling the temperature and time of burning so that maximum amorphous variety is produced. Patel et al. [16] informed that the temperature of carbonization was especially held below 700 °C to keep away any transformation of amorphous phase to crystalline form. The result showed that reheating ash to remove carbon residues took a relatively long period of time. In addition, high temperatures affected all amorphous silica to be converted to a crystalline form.

Both of rice husk ash forms have been widely used as catalysts and adsorbents [17]. It has been used as an active silica source because it is cheap, less selective, and highly active [18]. Rice husk ash has microporous crystals with intricate pores and channels after carbonization process as shown in Figure 2.2.

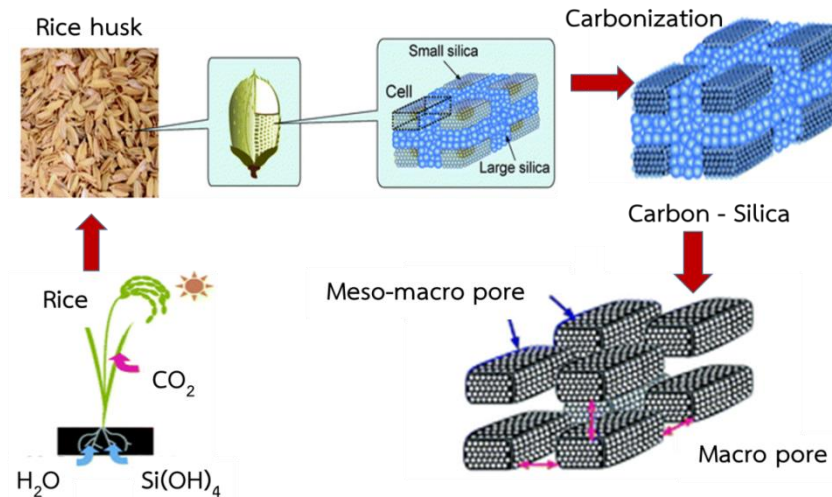


Figure 2.2 Porous carbon from rice husk [19].

2.2 Magnetic Materials

Magnetic materials are the mixed-metal oxides of formula MFe_2O_4 (M: divalent metals) with cubic spinel structure. The separation of magnetic materials can be realized in a few minutes using external magnetic field. Magnetic materials can be classified in term of magnetic properties such as paramagnetism, ferromagnetism, ferrimagnetism, antiferromagnetism and superparamagnetism.

2.2.1 Magnetic Properties

2.2.1.1 Paramagnetism

When the material is exposed to an external magnetic field and arrange in the same direction, dipole moments of paramagnetic material specially align by a rotation. Nevertheless, the dipole moment is still less than the highest possible value. “Paramagnetic” is the behavior of materials responding less in the same direction with a magnetic field. When an external magnetic field is removed, the alignment of magnetic dipole is lost.

2.2.1.2 Ferromagnetism

Ferromagnetic materials is the basic mechanism that is a permanent magnetic material. If the value of the exchange interaction is positive then ferromagnetism is to be expected. Moreover, these materials magnetized easily when exposed to strong magnetic field. These materials remain magnetized after the removal of an external magnetic field. Magnetic susceptibility of these materials is higher than that of paramagnetic materials. Ferromagnetic materials lose their magnetic properties when heated to Curie point; on the other hand, when cooled down, they exhibit ferromagnetic properties again. This state of affairs is found in only four elements, such as Iron, Cobalt, Nickel, and Gadolinium at room

temperature. Two lanthanides, Terbium and Dysprosium, have a temperature range (well below room temperature) over which they are ferromagnetic.

2.2.1.3 Ferrimagnetism

Ferrimagnetism is exhibited by ferrites and magnetic garnets. The oldest known magnetic substance, magnetite (Fe_3O_4), is a ferrimagnet. Ferrimagnet, a magnetic property, is also considered as the ferromagnetism unique case that it has magnetic dipoles alignments, but including opposite direction in some alignments. Hence, these objects found in some ionic compounds such as ceramic, oxides, or more complex forms presented spontaneous magnetization. Magnetite (Fe_3O_4), one of ferrites materials, is known for the ferrimagnetism. A ferrimagnet composes of two magnetic sublattices (called A and oxygen, reconciled for exchanging the interactions between the spinning of A and B sublattices. Both ferromagnetism and ferrimagnetism have same properties such as spontaneous and remanence magnetizations.

2.2.1.4 Antiferromagnetism

A special case of ferromagnetism can be called for this property. The magnetic dipoles of the antiferromagnetic materials prepared by themselves in an opposite direction of magnetic field, so the net dipole moment is zero. Manganese and chromium are some of these materials. The interaction between the d orbitals giving rise to the conflict between the exchange energy and the bonding energy does not operate so simply in many compounds. In these, the transition metal ions are separated by a nonmetal such as oxygen, and the compounds are antiferromagnetic.

2.2.1.5 Superparamagnetism

Superparamagnetism is a form of magnetism that appears in ferromagnetic or ferromagnetic nanoparticles. This behavior occurs by a reduction of the magnetic material domain into a single domain state in a particulate. Superparamagnetic materials behave like paramagnetic in that they have no permanent magnetic moment. In the absence of external magnetic field, their magnetization appears to be in average zero. In contrast, under an external magnetic field, the nanoparticles are readily magnetized.

2.2.2 Iron based magnetic particles

Magnetic material as iron ferrites are type of ceramic compounds derived from iron oxides mixed with metal oxide such as hematite (Fe_2O_3) or magnetite (Fe_3O_4). Figure 2.3 presents that several ferrites are spinels that have the formula of AB_2O_4 , where A atoms and B atoms represent various metal cations, with a cubic spinel structure. Structure of spinel can be divided into two types which are normal and inverse spinel. Firstly, normal spinel structure has A atoms occupying 1/8 the

tetrahedral holes and B atoms occupying 1/2 the octahedral holes. Second, if 1/8 of the tetrahedral holes are occupied by B cation, then 1/4 of the octahedral sites are occupied by A cation and the other 1/4 by B cation and that is called the inverse spinel structure [20].

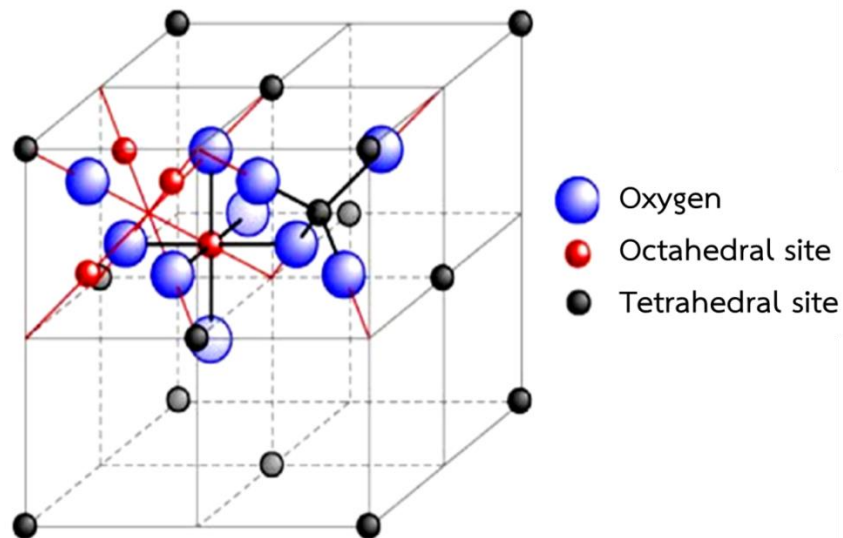


Figure 2.3 The two magnetic atoms A and B of a spinel structure [20].

Figure 2.4 presents the distribution of divalent and trivalent metals in the A and B atoms make spinel structures into normal spinel and inverse spinel structures. In a normal spinel, such as ZnFe_2O_4 , two Fe^{3+} cations per formula unit occupy B sites and one Zn^{2+} cation occupies the A sites. Inverse spinel structure possesses different distribution of metals as discussed in the next section.

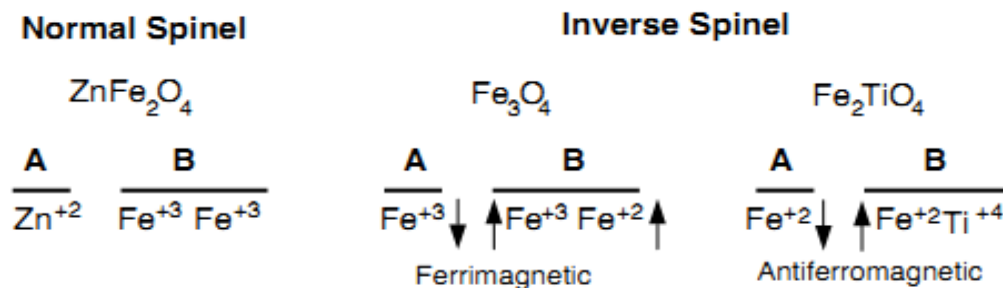


Figure 2.4 Cation distributions in normal spinel and inverse spinel. A and B indicate A atom and B atom cations, respectively [21].

2.2.2.1 Maghemite (γ -Fe₂O₃)

The maghemite has the same structure as magnetite but maghemite has the trivalent of Fe in the two sublattices. The unit cell of maghemite contains $21\frac{1}{3}$ of Fe³⁺ ions, 32 of O²⁻, and $2\frac{1}{3}$ vacancies. The vacancies exist in octahedral sites. The nature of precursor, the crystallite size and the amount of Fe²⁺ are related to the extent of vacancy ordering. The magnetic property of maghemite is also ferrimagnetism. The ferrimagnetism occurs by unequal distribution of ions in tetrahedral and octahedral sites. Maghemite is usually used in recording media due to its stability and low prices.

2.2.2.2 Magnetite (Fe₃O₄)

The magnetite (Fe₃O₄) is an inverse spinel magnetic material, A unit cell includes 16 Fe³⁺ and 8 Fe²⁺ cations. Magnetite formula may be written as (Fe³⁺)₈tet(Fe³⁺Fe²⁺)₈octO₃₂, which is B sites per formula unit are occupied by one of Fe²⁺ and Fe³⁺, and the remaining Fe³⁺ cations occupies the A sites as shown in Figure 2.5.

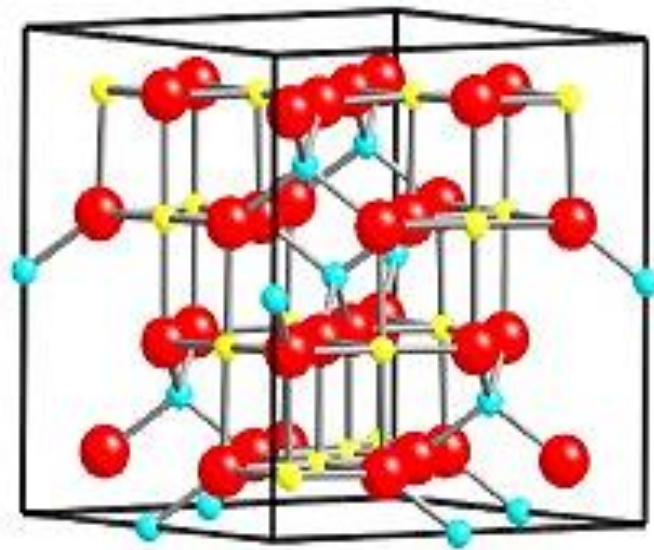


Figure 2.5 Chemical structure of (a) The inverse spinel Fe₃O₄ bulk unit cell containing O (red), tetrahedral Fe (A) atoms (*light blue*) and octahedral Fe (B) atoms (*yellow*) [22].

2.3 Polystyrene

Polystyrene, the most commonly used polymer in technological applications, has a very low surface energy and is hydrophobic. Polymer surface modifications are generally performed if the surface properties do not suit the desired applications. After modification the surface should carry the functional groups, while the bulk properties should remain unchanged.

Polystyrene (PS) is made from styrene monomers. In the polymerization that shows in Figure 2.6, the C-C pi-bond (in the vinyl group) is broken and a new C-C single (sigma) bond is formed, attaching another styrene monomer to the chain. The newly formed sigma bond is much stronger than the pi-bond that was broken, thus it is very difficult to depolymerize polystyrene. About a few thousand monomers typically comprise a chain of polystyrene, giving a molecular weight ranging from 100,000 to 400,000.

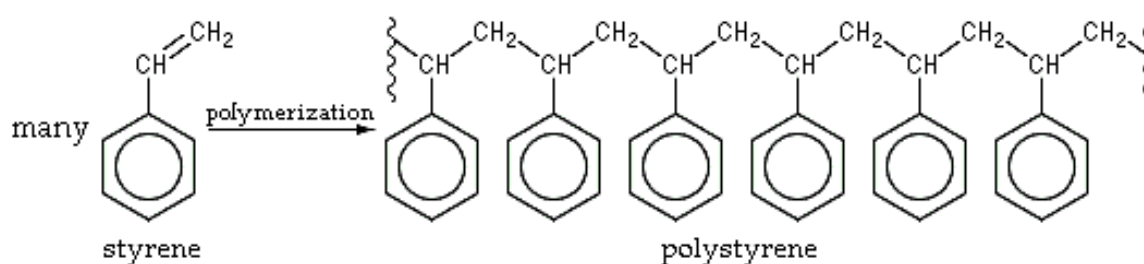


Figure 2.6 Chemical structure of polystyrene.

In this study, polystyrene foam (Styrofoam), the most commonly used polymer in technological applications such as a packing material, was selected and used. It has impact resistance and efficiency to be shaped and its thermal insulating properties which make it ideal to protect thousands of different products.

Moreover, polystyrene also has been chosen as recycled material due to the contribution towards non-biodegradable material when it exposes to the landfill. In addition, this waste will also create harmful to environment because its toxicity and recalcitrant compounds. Thermal degradation of foamed polystyrene was investigated by Mehta et al. [23]. Polymer collapses at 110-120°C, melts at 160°C, starts to decompose and vaporize at 275°C and completely volatilizes at 460-500°C. Table 2.3 shows that Styrofoam cannot be decomposed though using long period of time.

Table 2.3 Decomposition rates of natural and synthetic materials[24]

Source and process	Materials	Decomposition rates
Natural	Paper	2–4 weeks
	Leaves	1–3 months
	Orange peels	6 months
	Natural Milk Cartoon	5 years
Synthetic	Plastic bags	10–20 years
	Plastic container	50–80 years
	Aluminum can	80 years
	Tin can	100 years
	Plastic soda bottle	450 years
	Glass bottle	500 years
	Styrofoam	Never

Nevertheless, polystyrene has a very low surface energy and is hydrophobic material, which means that it is water rejective as shown in Figure 2.7. In aqueous solution hydrophobic domains try to hide from contact with water, e.g. by conformational change. When hydrophobic domains come in contact with the (hydrophobic) polystyrene surface they readily adsorb. Adsorption occurs through non-covalent interactions i.e. no chemical bonds are formed. These interactions are weak but the final strength depends on the number of interactions, which in turn depends on the size, number and position of the hydrophobic domains on the surface of the molecule.

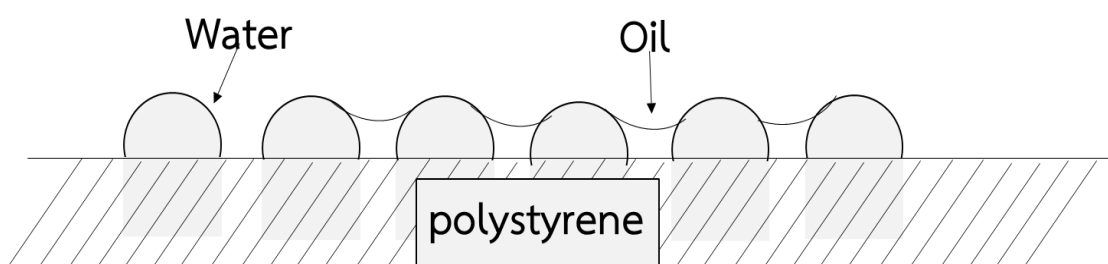


Figure 2.7 Schematic showing the spreading of oil on a polystyrene surface covered with water drops.

In using polymer to modify a surface of materials, Sun et al. [25] used polystyrene, because it is commonly low surface energy material in superhydrophobic surfaces. And Jinyou et al. [26] reported that nanoporous

polystyrene (PS) fibers were used as oil sorbent with highly porous structures. The fiber had ability to adsorb motor oil with the highest capacity of 113.87 g/g.

2.4 Crude oil

Crude oil is a very complicated composition that contains thousands of hydrocarbon and organic compounds. Each crude oil is a unique mixture, not matched exactly in composition or properties by any other samples of crude oil. Generally crude oil contains the classes of hydrocarbon and non-hydrocarbon compounds.

A) Hydrocarbon compound

Hydrocarbon compound consists of predominantly of alkanes, cycloalkanes and aromatic hydrocarbons covering the carbon number range from C1 to C60+.

(i) Alkanes (paraffins)

Alkanes are straight or branched chain have formula C_nH_{2n+2} . The lighter, straight-chain paraffin molecules are found in gases and paraffin waxes. The branched-chain (isomer) paraffins are usually found in heavier fractions of crude oil. Crude oil vary in alkanes content.

(ii) Cycloalkanes (naphthenes)

Cycloalkanes (or cycloparaffins) are saturated hydrocarbon groupings with the general formula C_nH_{2n} , containing structures with carbon atoms linked in a ring. Ring of cycloalkane with five and six carbon atoms predominate, with two-ring naphthenes (dicycloparaffins) is found in the heavier ends of naphtha. The cycloalkane composition in crude oil varies widely from 30% to 60% [20].

(iii) Aromatic hydrocarbon

Aromatic hydrocarbon are unsaturated ring-type compound such as, benzene, benzene derivatives and fused benzene ring compounds. Benzene in crude oil has been reported to range between 0.01% and 1%. Also, polycyclic aromatic hydrocarbon (PAH) are most abundant of the main hydrocarbons found in crude oils and they can be carcinogenic to plants and animals [21].

B) Non-hydrocarbon compounds

(i) Sulfur compounds

Crude oils varies widely in sulfur content, which can range from 0.1 % to 10% by weight, and it may be present in crude oil as hydrogen sulfide, thiols (mercaptans), sulfides, disulfides and thiophenes [22]. These are corrosive substances. Moreover, the corrosive sulfur compounds have an obnoxious odor.

(ii) Nitrogen compounds

Nitrogen is found in lighter fractions of crude oil as basic compounds. The nitrogen content of crude oils ranges from trace amounts to 0.9% by weight.

The decomposition of nitrogen compounds in catalytic cracking and hydrocracking processes forms ammonia and cyanides that can cause corrosion.

(iii) Oxygen compounds

Oxygen compounds such as phenols, ketones, and carboxylic acids occur in crude oils in varying amounts from 0.06-0.4%. The majority components are alkane and cycloalkane (naphthenic) acids. Other minor components include ketones and phenols [22]. The oxygen content of crude oils increases with boiling range, so that more oxygen-containing compounds are found in distillates that boil above 400°C.

(iv) Heavy metal-containing compounds

Traces of several metallic compounds can be found in crude oils. Metals in crude oil, including nickel, iron, and vanadium are often found in small quantities, which have been identified in crude oils at levels ranging from a few parts per million to 200 ppm (mg/kg) nickel and up to 1200 ppm (mg/kg) vanadium [22].

2.4.1 Toxicity of crude oil

Chemical compositions commonly found in crude oil consist of alkanes, benzene, ethyl benzene, xylene, naphthalene, methylnaphthalene, toluene, and hydrogen sulfide. Local Poison Control Centers and Health Departments, and several federal agencies, for example the USEnvironmental Protection Agency (EPA) [23], are tracking calls related to potential exposures to this chemical. Routes of exposure and absorption can be inhaled, consumed in contaminated food or water, absorbed through the skin, or ingested through contaminated water. The anthropogenic high hydrocarbon concentrations of introduction into the marine environment can either kill or cause lethal effects in several sub marine life forms, plant and human economic activity. The effects resulting from exposure to crude oil can range from biochemical to organismal in scope.

2.4.1.1 Acute (immediate) health risks

Briefly exposures at relatively high levels to moderate levels in a short term can cause confusion, weakness, impaired memory or motor control, nausea, loss of appetite, loss of hearing and color vision. Crude oil can make skin irritation and mucous membranes on contact. Irritant effects may range from a slight reddening of the skin to burning, swelling, pain and permanent skin damage. Common effects from acute exposure to crude oil through inhalation and ingestion are difficulty breathing, headaches, dizziness, nausea, confusion and other central nervous system (CNS) effects.

2.4.1.2 Chronic (long-term) health risks

At any possible long term exposure at relatively low levels should be avoided because of the possibility of serious effects to organs such as lung, liver and kidney damage, infertility, immune system suppression, disruption of hormone levels, blood disorders, gene mutations and cancer.

2.4.2 Contamination of oil

There are mainly three ways that oil leaks, occurred by several causes, affect environment: air, land and water.

2.4.2.1 Oil contamination in air

Air is not contaminated by oil directly, but the volatile organic compounds (VOCs), the lightest hydrocarbon of crude oil can evaporate into air. Normally gasoline can evaporate easily. The volatile is 1,2,4-trimethylbenzene (TMB) which is a crucial product in a petroleum refinery distillation or about 40% that is C9 aromatic. Almost refineries make C9 fraction to gasoline [27]. A part of heavy atmospheric contamination, rare compounds takes days to evaporate. Moreover, burning oil makes carbon dioxide and carbon monoxide, which cause toxicity in air.

2.4.2.2 Oil contamination in land

There are several garages that used to repair car, motorcycle, truck, etc and oil can be dispersed on land. Waste oil is also essential to be proceeded the solution. Furthermore, the accidental oil spills, leaks, or discharges are risk to petroleum contamination. Oil covers over soil that make water cannot insert to soil. Absorption, transferring and replacement of oil contaminated in soil are costly because removing an oil spill or contamination from soil is hard to resolve this problem. There are many methods to solve this problem for example, steam/air stripping, encapsulation, chemical treatment, bioremediation, etc [28]. Impacts of oil spills on land it is crucial to have knowledge not only of the surface effects but also of the sub-surface perseverance of the soil, its chemical transformations and its transport in groundwater [29].

2.4.2.3 Oil contamination in water

One important way to contaminate in water, mainly occurred by human activity is particularly marine transfer of oil. The oil spill is discharged of liquid petroleum to environment. Then, crude oil is spilled in the sea, it spreads rapidly to other areas by ocean current so it is hard to pick up and clean [30]. Spilled oil weathers and becomes emulsified by physically incorporating water droplets into it. The process forms a stable mixture. Most crude oils and heavier refined products form emulsions with varying water content. Subsequently, emulsification will increase the volume of contaminant to manage. There are several processes to

remedy oil contamination. Clean up oil spills procedures have to be considered to use mixed methods to lower risk to environment [31].

2.4.3 Removal of crude oil and treatment of oil spill

2.4.3.1 Mechanical techniques

Using booms to prevent oil slicks spreading is one of mechanical techniques. Booms are conjunct with skimmer for carrying out concentrated oil [32]. Booms are used in concentrating oil with sufficiently thick layers on the water from spreading because of easy disposal and treating, on the other hand these techniques are particularly affected by wind, wave and current. Furthermore, it also protects bays and beaches from oil [27].

Broje et al. [33] studied a used of skimmers to keep oil on several factors for example; oil slick viscosity, thickness, and oil slick temperature. Sweeping of oil by skimmers is slow but they are very effective machines used for surface removal in calm or sheltered waters and along shorelines. They worked by taking advantage of high slick viscosity and thickness also increases recovery efficiency and the adhesive nature of the oil, which will cling to any surface that it comes into contact with.

2.4.3.2 Bioremediation

Bioremediation is an application to cleanup oil on the water. That involves the biological agents, such as fertilizers-nutrients to microorganism in the contaminated area so as to degrade oil for example bacteria, fungi, and yeast. Thus this method is not widely applied to oil spill [34].

2.4.3.3 Dispersants

Dispersants are widely applied to cleanup oil spillage. This method designed to spread oil because it can be used in light to medium weight oil. When it is sprayed on oil spillage, the dispersants that use to break oil into the droplets and reduce interfacial tension between oil and water by emulsification [35]. But the droplets spread into the water and it will be toxic to aquatic animal at the sea bed [31]. Nevertheless, it can be treated in large areas compared to other methods.

2.4.3.4 Sorbents

Sorbents are products or materials used to dispose oil from water surface or land that are hydrophobic. Suitable sorbents should have high capacity to adsorb oil but also repel water in very small spill area where skimmer cannot be used. They have high capacity to absorb oil and repel water [36]. Literature review showed that natural sorbents can serve better to absorb oil from the water surface than synthetic sorbents. In general term it can be separated to three mechanisms; absorption, adsorption or using both of them.

(a) Inorganic materials

Inorganic materials, known as sinking absorbents are highly dense and fine grained mineral materials either natural or processed used to sink floating oil. The instances are stearate-treated chalk and silicone-treated pulverized fly ash, zeolites, graphite, activated carbon, organoclay, silica (sand) and silica gel [37,38]. Because they have numerous shortcomings such as sea beds contamination and hazard effects to aquatic habitats. They incline to release some absorbed oil due to low retention capacity of some of the solids [32]. Furthermore they are very expensive adsorbents so that they are not commonly used.

(b) Synthetic organic products

They mainly consist of sorbents made from high molecular weight polymers for example polypropylene, polyethylene and polyurethane. Synthetic sorbents are available under various trade names and have good hydrophobic and oleophilic properties. They have high adsorption capacity such as ultralight, open-cell polyurethane foams can absorb 100 times of their oil weight from oil-water mixtures and ultralight [33]. Therefore, they are easier to recover and cheaper than some natural sorbents.

2.5 Literature review

2.5.1 Treatment of oil spill using adsorption process

Masomeh et al. [39] studied organically modified nanoclay (organoclay) prepared by exchanging the hexadecyltrimethylammonium bromide (HDTMA) with sodium ions in a montmorillonite structure. The structure was tested about petroleum hydrocarbon adsorption. The sorbent materials for sorption of products that are involved in oily wastewaters and land-based oil spills was investigated for the effectiveness of adsorption using crude oil, kerosene, gasoline and toluene. The process parameters such as sorbent dosage and contact time were valuated. The results presented that adsorption capacity of the organoclay was clearly higher than the capacity of unmodified clay. The results in a process were also showed that the adsorption capacity was in the range of 4 to 10 gram per gram of adsorbent depending on the hydrocarbons and the adsorption equilibrium was also attained within 1 hour.

Sokkera et al. [40] synthesized adsorbent of crude oil removal (initial concentration 0.5–30 g/L) from aqueous solution by using hydrogel of chitosan based polyacrylamide (PAM). Polyacrylamide obtained by radiation induced graft polymerization has been examined. The experiments were performed with different initial concentrations of oil residue, acrylamide concentration, contact time and pH to find out the optimum condition to adsorp residual oil from aqueous solution and

sea water. The results showed that the hydrogel prepared with a concentration of 40% acrylamide (AAm) and at a radiation dose of 5 kGy has high removal efficiency of crude oil of 2.3 g/g at pH 3. Also equilibrium studies have showed the capacity of adsorption of crude oil of the hydrogel.

2.5.2 Preparation of rice husk ash and its chemical modification

Singh et al. [41] reported an obtained silicon of 99.9999% purity by using magnesium to reduce white rice husk ash at temperature of 800 °C. Then, using many successive acid leaching treatments (mixtures of HF, H₂SO₄ and HCl) at temperatures of 850-900 °C was recorded the reduction of white rice husk ash. The silica in their rice husk was investigated to have attained some degree of crystallinity when firing lower than 800 °C. They also recommended the possibility of obtain silicon of similar purity by directly smelting the purified amorphous silica with carbonaceous reductants in electric furnace, then followed by leaching with acids and repeating the smelting and leaching for about nine times.

Sun et al. [25] studied polystyrene/silica nanoparticles, which were prepared by radical polymerization of silica nanoparticles possessing vinyl groups and styrene with benzoyl peroxide as an initiator. The result of vinyl silica nanoparticles and polystyrene/silica nanoparticles was identified by means of Fourier transform infrared spectroscopy, scanning electron microscopy and UV-vis absorption spectroscopy. From the results, polystyrene had been successfully grafted onto vinyl silica nanoparticles via covalent bond. The morphological structure from polystyrene/silica nanoparticles film, examined by scanning electron microscopy, indicated a rough structure attribute. The surface wetting properties, those of the polystyrene/silica nanoparticles film, were evaluated by measuring the water contact angle and the sliding angle using a contact angle goniometer. The contact angles of water drops on film were 159° and 2°, respectively. The outstanding superhydrophobic property expands the potential applications of the superhydrophobic surfaces.

Kim et al. [42] synthesized Fe₃O₄ nanoparticles having a size of 10 nm by the co-precipitation of Fe³⁺ and Fe²⁺ at a ratio of 2:1 with NH₄OH under nitrogen atmosphere. The Fe₂O₃ was prepared by co-precipitation and sol-gel process using Fe(NO₃)₃·9H₂O and ethylene glycol. Silica particles were coated with Fe₃O₄ by the hydrolysis of tetraethyl orthosilicate (TEOS) and 2-aminopropyltriethoxysilane (2-APTES). That process appeared Fe-O-Si chemical bonds in the surface of the magnetic nanoparticles.

Dong et al. [43] reported a novel type of composite microspheres exhibiting magnetic properties. The composite microspheres consisted of Fe₃O₄, silica, and poly(c-benzyl-L-glutamate) (PBLG). To prepare the composite microspheres, Fe₃O₄

nanoparticles were manufactured using the solvothermal method and then coated with a silica shell by tetraethoxysilane. Accordingly, amino groups were added on the above Fe_3O_4 -silica spheres using 3-aminopropyltriethoxysilane. Eventually, the obtained spheres were used as initiator for polymerizing *c*-benzyl-L-glutamate N-carboxyanhydride (BLG-NCA), providing the anticipated magnetic composite microspheres. They presented a high saturated magnetization of 34.1 emu/g and the anticipated rapid magnetic responsiveness

2.5.3 Utilisation of rice husk and rice husk ash as sorbents

Nwankwere et al. [44] have studied acetylated rice husks (ARH) as crude oil sorbents. Sorption kinetics and isotherms studies were operated under various experimental conditions for example, testing the experimental data with the pseudo-second-order kinetic model adsorption was therefore monolayer and the optimum theoretical monolayer sorption capacity was 10.31 g/g rice husks. These values indicated that the acetylated rice husks suitable sorbents with potential for further development for oil spill treatment.

Seiji et al. [45] studied that rice husks, as agricultural waste, are converted into adsorbent for intended use in oil spills disposal. The raw and refined (defiberized) husks of Japanese Akita Komachi rice were pyrolyzed in a vacuum (500 Pa) at 300–800 °C. Then, the amounts of heavy oils adsorbed on the carbonized rice husk were evaluated. Oil adsorption is relied on the type of oil. Rice husks were refined and then pyrolysed at 600–700 °C (1.0 g) with adsorption >6.0 g of B-heavy oil and <1.5 g of water, These indicated the usefulness as an adsorbent for oil spills cleanup in Japan. The refining process contributed to an improvement in the oil adsorption capacity with the carbonization time (at 600°C) has only a minor effect on oil adsorption. Instead of their porosity and the residual fluid components in the carbonization step, rice husks are closely related to oil adsorption capacity.

Uzunov et al. [46] reported oil sorption capacity by using adsorbents, pyrolysed rice husk at different temperatures ranging from 250-700 °C. Received rice husk ash had dissimilarity of volatile compounds and contained different functional groups. When increasing the pyrolysis temperature, the amount of fluids increased, but their diversity decreased. The pyrolysed temperature at 480°C has a maximum solid residue and amount of macropores, which affected the sorption of oil.

Kenes et al. [47] studied thermally treated rice husks, which mainly consisted of amorphous SiO_2 leading to an examination of petroleum sorption capacity. The results showed that prepared rice husks at 700 °C were able to adsorb petroleum at the maximum of 9.2 g/g. The petroleum sorption capacity of thermally treated rice husks depended on heating temperature, contact time and petroleum density due to the basis of phase composition, microstructure and morphology.

According to the literature reviewed above, rice hush ash is a very promising porous material for oil adsorption applications due to high amount of production and low cost and high surface area. Thus in this research, rice hush ash was used as a supported material for oil adsorption. Its magnetic property will be enhanced in order to facilitate the separation by external magnetic field, as well as its hydrophobic property will be improved by polystyrene coating.

CHAPTER III
EXPERIMENTAL

3.1 Instruments

The analytical instruments used for characterizations and measurements in this thesis are shown in the Table 3.1

Table 3.1 List of analytical instruments

Instruments	Manufacture: Model	Purpose
1. X-ray fluorescence (XRF)	Philips, model PW 2400	Quantitative chemical analyses of RHA
2. CHNS/O analyzer	Perkin-Elmer: model 2400II	Determination of carbon, hydrogen, and nitrogen in the adsorbents
3. Atomic absorption spectrometer (AAS)	Perkin-Elmer, Analyst 300	Determination of Fe of extracted RHA/Fe ₃ O ₄
4. X-ray diffraction (XRD)	Rigaku DMAX2200/Ultima ⁺	Crystallinity study
5. Contact angle goniometer	Ramé-Hart, model 100-00	Measurement of the dynamic advancing and receding water contact angles
6. Scanning Electron Microscope/ Energy-dispersive X-ray spectrometer (SEM/EDX)	JSM-5800LV and link ISIS Series 300	Imaging of the RHA, composites and elemental analysis
7. Surface area analyzer	BEL Japan: BELSORP-mini	Surface area measurement
8. Fourier transform infrared spectrometer (FT-IR)	Nicolet Instruments Technology: Impact 410	Functional group identification
9. Thermogravimetric analyzer (TGA)	Perkin-Elmer: Pyris1	Study of thermal stability of the adsorbents

3.2 Chemicals

The solvents and reagents in all experiments are summarized in Table 3.2

Table 3.2 Chemicals and suppliers

Chemicals	Suppliers/ Grade
Toluene	Merck. Germany / for analysis
Acetone	Fisher Scientific, England / A.R.
Hydrochloric acid 37%	Merck. Germany / for analysis
Sulfuric acid 97%	Merck. Germany / for analysis
Nitric acid 65%	Merck. Germany / for analysis
Sodium hydroxide	Merck. Germany / for analysis
1-octadecene	Merck. Germany / for analysis
Iron (III) chloride	Sigma-Aldrich / A.R.
Iron (II) chloride tetrahydrate	Fisher Scientific, England / A.R.

3.2.1 Preparation methods of chemicals and reagents

All solutions were prepared by using deionized (DI) water.

3.2.1.1 Sodium hydroxide solutions

Sodium hydroxide solutions (1 M) were prepared daily by dissolving the appropriate amount of NaOH in deionized water.

3.2.1.2 Nitric acid solutions

Nitric acid solutions (1 M) were prepared daily by direct dilution from the concentrated solution (65%).

3.2.1.3 Hydrochloric acid solutions

Hydrochloric acid solutions (0.5, 1 M) were prepared daily by direct dilution from the concentrated solution (37%).

3.3 Preparation of Rice husk ash

Rice husk was washed with water to remove the soluble particles and then dried in an oven at 110 °C for 8-10 hours. Rice husk ash was prepared according to the publication of Liou [1]. Hydrochloric acid leaching was used in the extraction of inorganic impurities from the rice husk. For the first step, 100 g of rice husk was treated with 1 L of 1 M HCl for 2.5 hours and refluxed for 2.5 hours with continuous stirring. The pretreated rice husk was washed several times with deionized water and dried at 120 °C for 12 hours. The rice husk was placed in porcelain crucibles and calcined at different temperatures of 500, 600, and 700 °C for 1 hour in a

closed electric muffle furnace and allowed to cool in the furnace. Figure 3.1 shows the pictures of rice husk and the prepared rice husk ash.



Figure 3.1 Rice husk and prepared rice husk ash.

3.4 Preparation of RHA/Fe₃O₄

The RHA/Fe₃O₄ was synthesized by the co-precipitation of FeCl₃ and FeCl₂ salts. In this step 0.324 g of FeCl₃ (2 mmol) and 0.127 g of FeCl₂·4H₂O (1 mmol) were dissolved in a beaker which contained 10 mL of 0.5 M HCl. While stirring the reaction mixture, 8 mL of 1 M NaOH was gently added dropwise into the solution and then 1 g of rice husk ash (RHA) was added. After stirring for 3 hours, the black precipitate in the beaker was instantly formed. The RHA/magnetite precipitate was washed several times with deionized water and then dried in an oven at 110 °C for 12 hours. Finally, RHA/Fe₃O₄ composites were obtained.

The content of Fe₃O₄ in RHA/Fe₃O₄ composite was determined by atomic absorption spectrometry. The Fe₃O₄ attached in RHA/Fe₃O₄ composite was extracted. Solution of 50 mL of nitric acid and hydrochloric acid with a volume ratio of 1:3 was added to 10 mg RHA/Fe₃O₄, the mixture was heated at 90-95 °C until there was no more brown fumes. The mixture was further heated until almost dry. Then, the standard method for digestion of sediment, sludges, and soils (EPA Method 3050 B) was applied to extract Fe ions from RHA/Fe₃O₄ as follows:

- 1) Solution of 5 mL conc. HNO₃ and DI water with a volume ratio of 1:1 was added to the mixture with continuous heating at 90-95 °C for 15 minutes.

- 2) Conc. HNO₃ (2.5 mL) was added and the mixture was heated for 30 minutes. This step was repeated again.

- 3) The mixture was heated until the total volume was around 5 mL and then cooled down.

4) DI water (2 mL) and 30% H₂O₂ (3 mL) were added into the mixture and heated gently to prevent the mixture from boiling over.

5) 30% H₂O₂ (1 mL) was added to the mixture each time and the total volume of 30% H₂O₂ was 7 mL.

6) An aliquot of 2.5 mL of conc.HCl and 5 mL of DI water were added. The mixture was heated to reflux for 15 minutes and then, wait until it cooled down.

7) The solution was transferred into a 100 mL volumetric flask and made up to mark with DI water.

8) The mixture was filtered using a membrane filter. The solution containing Fe ions was obtained.

Concentrations of Fe ions in the solution were determined by atomic absorption spectrometry (AAS).

3.5 Preparation of RHA/Fe₃O₄-PS composite

As-synthesized RHA/Fe₃O₄ composites (1 g) was mixed with a solution of polystyrene (0.05, 0.10, 0.15 g), which was previously dissolved in toluene (10 mL). The resultant mixture was dried in an oven at 160 °C for 6 hours. The oven was kept at this temperature until the samples turned dark brown (6 hours). The synthesized composites were kept in a desiccator. All the composites obtained from each step were characterized by Fourier transform infrared spectrometry (FTIR), scanning electron microscopy (SEM) and thermogravimetric analysis (TGA).

3.6 Characterization of the materials

3.6.1 X-ray fluorescence (XRF)

Quantitative chemical analysis of the calcined rice husk at different temperature (500, 600, 700 °C) were accomplished by X-ray fluorescence (Philips, model PW 2400, The Netherlands).

3.6.2 CHNS/O Analyzer

Total carbon content of the calcined rice husk at different temperature (500, 600, 700 °C) was measured by CHNS/O Analyzer (Perker-Elmer Elemental analyzer, model 2400II)

3.6.3 Atomic absorption spectroscopy (AAS)

The determination of extracted Fe from RHA/Fe₃O₄ composite was accomplished by atomic absorption spectroscopy (Perkin-Elmer, Analyst 300).

3.6.4 X-ray diffraction (XRD)

The XRD patterns of the prepared composites were obtained from a Rigaku D/MAX-220 Ultima+ X-ray diffractometer (XRD) equipped with CuK α radiation (40 kV

30 mA) and a monochromator at 2 theta angle range of 10 to 80 degrees. The characterization and identification of crystalline structures were confirmed with the help of data files presented by Joint Committee on Powder Diffraction Standard (JCPDS).

3.6.5 Contact angle

The wettability of the composites was tested by measuring the contact angle of a drop of water on the surface of the composites. For each measurement, a photograph of the droplet was taken and a contact angle was measured directly from the photographic image. The composites were ground into powder for experiments of the polarity of the surface measurements.

3.6.6 Scanning Electron Microscope/ Energy-dispersive X-ray spectroscopy (SEM/EDX)

Particle morphology of composites was obtained using a scanning electron microscope (SEM, JSM-5800LV and Link ISIS Series 300). The EDX analysis allows to quantify the amount of Fe (as Fe_3O_4) in the material. The distribution of magnetic particles was also studied by elemental mapping method using energy dispersive X-ray (EDX) spectrometer equipped with the SEM.

3.6.7 Nitrogen adsorption (BEL Japan BELSORP-Mini).

The specific surface area and pore volume of the adsorbents were determined by BET (BEL Japan, BELSORP–mini instrument). The adsorbent weight was 20 mg and pretreated at 400 °C for 3 hours before each measurement. The principle of this method is the physical adsorption of a gas molecular species on a surface of adsorbent. Based upon one adsorbed layer, the quantity of adsorbed material gave directly the total surface area of the sample.

3.6.8 Fourier transform infrared spectroscopy (FT-IR)

The solid samples were prepared by pressing the sample with KBr. Infrared spectra were recorded between 400 to 4000 cm^{-1} . The Fourier transform Infrared model (Nicolet Instruments Technologies, INC. WI, USA) was used to identify the functional group of polystyrene-modified on the RHA/ Fe_3O_4 composite surface.

3.6.9 Thermal analysis

The thermograms of composites were measured using thermogravimetric analyzer: Pyris 1 (Perkin Elmer). Each composite was tested under the condition of 20°C/min heating rate under nitrogen atmosphere and over a temperature ranging from 25 to 800°C to determine the percentage weight loss at different temperature that can indicate the composition in RHA, RHA/ Fe_3O_4 and RHA/ Fe_3O_4 -PS composite.

3.7 Oil adsorption experiments

For the evaluation of the oil adsorption, the American Society of Testing and Materials (ASTM) F726-99 method was used and adapted as follows. A sintered glass crucible No. 4 was placed in a beaker filled with water at half level of the sintered glass height. Crude oil was then dropped onto the water surface in the sintered glass until the entire water surface was covered by crude oil thin film. 0.1 g of RHA/Fe₃O₄-PS composites was placed on the film of crude oil. Then the crucible was taken out from the beaker, and placed on a suction flask. Excess oil was removed by a suction pump. The initial and final weights of crucible and RHA/Fe₃O₄-PS composites were recorded. The effect of adsorption time was also studied by varying the contact times of 10, 20, 30 and 40 minutes. All experiments were done in triplicate. The oil adsorption capacity has been estimated at room temperature according to ASTM F726-06. The oil sorption capacities were calculated from the equation [48]:

$$Q = \frac{m_0 - m_s}{m_s} \quad (1)$$

where Q is the weight uptake of oil, m_s is the initial weight of the RHA/Fe₃O₄-PS composites and m_0 is the weight of RHA/Fe₃O₄-PS composites after sorption.

CHAPTER IV RESULTS AND DISCUSSION

In this study, composites of RHA and Fe_3O_4 particles were synthesized. Then the surface of RHA/ Fe_3O_4 composites was coated with polystyrene foam waste and the capability for oil removal was evaluated.

4.1 Characterization of the materials

4.1.1 X-ray fluorescence (XRF)

The chemical constituents of ash samples measured by X-ray fluorescence was shown in Table 4.1. The amounts of minerals in silica achieved by acid washing of rice husk and calcined at 500, 600, 700 °C were 50.69, 56.48, 64.90 % by weight respectively. The results showed that other substances such as Al_2O_3 and K_2O were found in trace amount (<0.15%).

Table 4.1 Chemical composition of RHA by XRF analysis

Substance	% mass		
	Ash calcined at 500 °C	Ash calcined at 600 °C	Ash calcined at 700 °C
SiO_2	50.69	56.48	64.90
Al_2O_3	0.06	0.13	0.09
P_2O_5	0.02	0.02	0.04
K_2O	0.03	0.04	0.05
CaO	0.01	0.02	0.02
TiO_2	0.01	0.01	<0.01

According to the results from Table 4.1, it shows that the ash calcined at 700 °C contains the highest amount of silica, but in the ashes produced at lower temperature, silica content decreased from 64.90% (700 °C) to 56.48% (600 °C). This can be explained by the fact that higher temperatures cause the thermal decomposition of organic constituents in the RHA. Increasing in percent of silica content will enhance the oil sorption capacity because amorphous silica has high surface area [49].

4.1.2 CHNS/O elemental analysis

CHNS/O elemental analysis results of ashes from rice husk prepared at various temperatures showed that carbon content is the most abundant component. Analytical characteristics are provided in Table 4.2. The carbon contents of rice husk

calcined at 500, 600, 700 °C were 36.32, 34.04, 22.47 % by weight, respectively. The acid pretreatment could remove impurities such as dust. After carbonization at high temperature (700 °C), the ash has low carbon content (22.47 %) because the thermal decomposition of organic contents has lower than the RHA calcined at 600 °C. However, the carbon content in ashes calcined at 600 °C and 500 °C was not significantly different.

Table 4.2 Chemical composition of rice husk ash by elemental analysis

%mass	Ash calcined at 500°C	Ashcalcined at 600°C	Ashcalcined at 700°C
Carbon	36.32	34.04	22.47
Hydrogen	1.85	1.37	1.24
Nitrogen	0.33	0.29	0.30

However, this study needs a material contained high silica and carbon content because a material composed of relatively high carbon proportion could be effectively used as the precursors of adsorbent synthesis, the carbon-rich ash might be easier to be coated with polystyrene. From the result in Table 4.2, the material prepared at 500 °C has the highest amount of carbon and that of 600 °C has slightly lower carbon (~2%). Therefore, regarding silica and carbon content (the total content of these two components of more than 90% by weight), the most preferred condition for ash preparation is at 600 °C.

4.1.3 X-ray diffraction technique

The crystallinity of the RHA, calcined at 600 °C, was determined by X-ray diffraction analysis. The XRD pattern of RHA (Figure 4.1) shows the characteristic peak centered at 2 theta range of 15 to 70 degree. The X-ray diffractogram of RHA showed a broad peak appeared around 2theta equal to 22 degree [50], which is a characteristic of amorphous structure of silica which is similar to the information given by JCPDS standard (JCPDS No.82-0512).

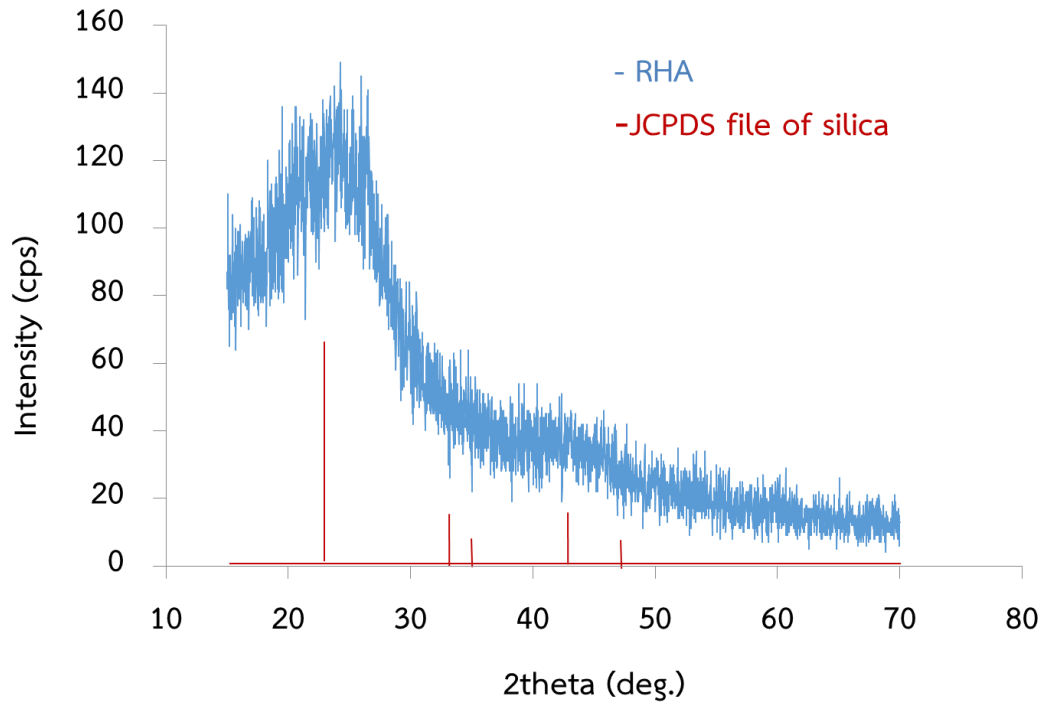
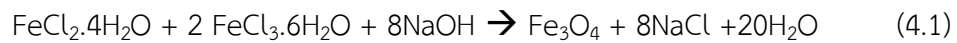


Figure 4.1 X-ray diffraction pattern of RHA compared to JCPDS pattern of silica.

Magnetic precipitate (Fe_3O_4) was synthesized by chemical co-precipitation of FeCl_3 and FeCl_2 , using a step procedure according to equation 4.1.



The crystal structure of Fe_3O_4 particles was confirmed by the XRD pattern shown in Figure 4.2, the diffraction peaks at 30.5, 36.5, 43.5, 53.7, 57.0 and 62.8° degrees correspond to plane reflection of Fe_3O_4 (220), (311), (400), (422), (511) and (440), respectively [51]. This pattern was confirmed that the precipitate was magnetite (Fe_3O_4) by comparing with the literature (JCPDS card file no. 19-0629).

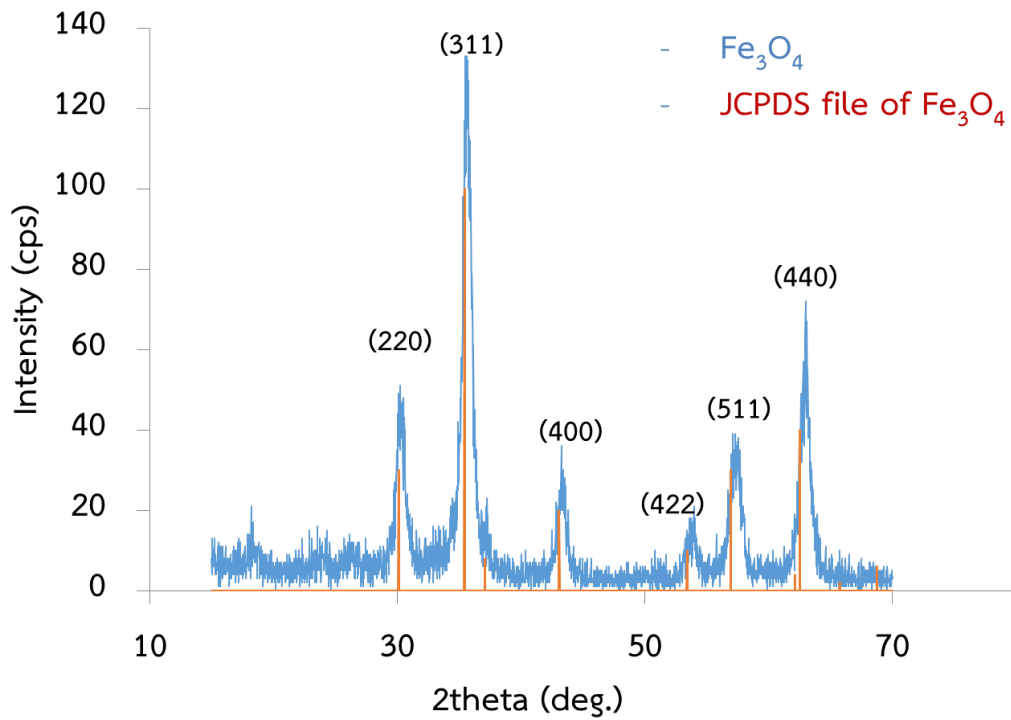


Figure 4.2 X-ray diffraction pattern of Fe₃O₄ compared to JCPDS pattern of Fe₃O₄.

The XRD pattern of RHA and RHA/Fe₃O₄ was compared and shown in Figure 4.3. The diffraction angle region of 2 theta ranging from 15 to 70 degree shows strong Fe₃O₄ spinel structure diffraction peaks at 36.5, and 62.8° with the broad diffraction peak of amorphous silica at 22°. This result illustrates the presence of the magnetic particles on the composite that was mainly magnetite (Fe₃O₄) crystalline by comparing with the literature [51].

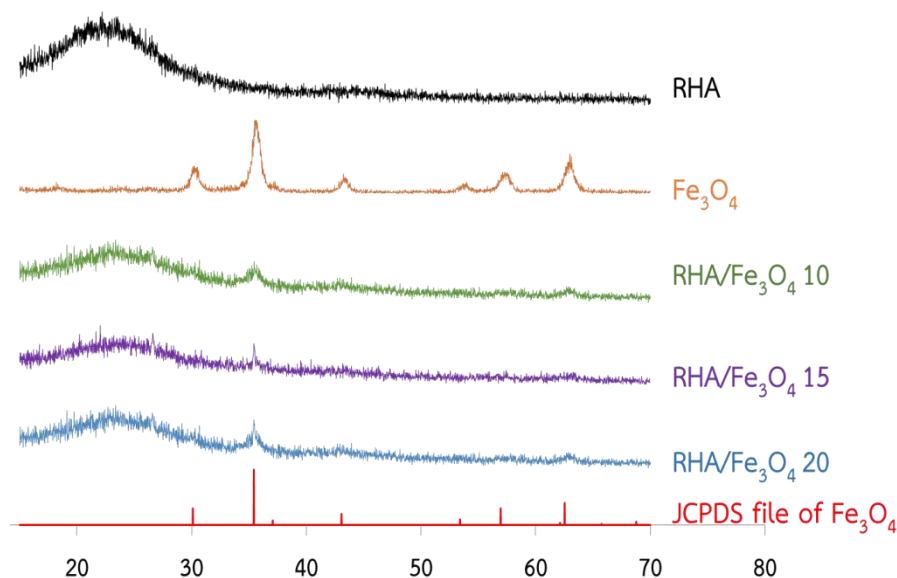


Figure 4.3 X-ray diffraction pattern of RHA, Fe_3O_4 , $\text{RHA}/\text{Fe}_3\text{O}_4$ composites and JCPDS file of Fe_3O_4 (No. 19-0629).

The average crystallite size of Fe_3O_4 on the composites can be calculated from the full-width at half maximum (FWHM) at the strongest diffraction peaks of $\text{RHA}/\text{Fe}_3\text{O}_4$ ($2\theta = 36.5^\circ$) using Debye–Scherrer formula as shown below [53]:

$$D = \frac{K\lambda}{\beta \cos\theta}$$

Where λ is the wavelength of the X-ray radiation ($\lambda = 0.15418$ nm), K is the Scherrer constant ($K=0.89$), θ is the characteristic X-ray radiation and λ is the full width at half maximum (FWHM) in radians in the 2θ scale. However, the crystallite sizes reported here were obtained using the software which estimates the sizes from the XRD patterns of the composites after the subtraction of the background from RHA. Based on the XRD results, the crystallite sizes of $\text{RHA}/\text{Fe}_3\text{O}_4$ 10%, $\text{RHA}/\text{Fe}_3\text{O}_4$ 15% and $\text{RHA}/\text{Fe}_3\text{O}_4$ 20% were calculated to be 7.5, 15.2 and 22.7 nm, respectively.

4.1.3.1 The effect of Fe_3O_4 amount

Various quantities of Fe_3O_4 of 10, 15, and 20 percent of RHA weight was investigated in the synthesis of $\text{RHA}/\text{Fe}_3\text{O}_4$ composite. The magnetic content in RHA was determined after extraction of 10 mg composite using 100 mL acid solution.

The extracted Fe in the solution was determined by FAAS. The amount of magnetic composition observed in the composite was calculated as shown in Table 4.3.

Table 4.3 Amount of Fe_3O_4 observed in the RHA/ Fe_3O_4 composites

Fe_3O_4 added (mmol/g composite) (% added)	Size (μm)	Observed amount of Fe_3O_4 (mmol/g composite)	% incorporated Fe_3O_4^*
0.4185 (10%)	1-75	0.089 \pm 0.007	21.3
	75-150	0.114 \pm 0.005	27.2
0.5996 (15%)	1-75	0.106 \pm 0.006	17.6
	75-150	0.129 \pm 0.010	21.5
0.7640 (20%)	1-75	0.119 \pm 0.003	15.6
	75-150	0.136 \pm 0.007	17.8

*Percentage of incorporated Fe_3O_4 in the composite comparing with starting (added) Fe_3O_4 .

Based on the result in Table 4.3, the result showed that the observed amount of Fe_3O_4 in the RHA/ Fe_3O_4 composites slightly increased when increasing the initial amount of starting material for Fe_3O_4 preparation. The percentage of added Fe_3O_4 of 20% showed the maximum deposition of Fe_3O_4 on RHA of 0.119-0.136 mmol/g. According to the percentage of incorporated Fe_3O_4 in the composite comparing with starting (added) Fe_3O_4 , the composite prepared by 10% of Fe_3O_4 showed the highest incorporation percentage of about 21.3 and 27.2. On the other hand, when Fe_3O_4 was increased on the surface of RHA, the surface area decreased (see Table 4.4). Only 10% of starting Fe_3O_4 was enough to make the composite respond to the magnetic field (see Figure 4.15). Moreover, the composite of 10% of starting Fe_3O_4 has the highest surface area.

4.1.4 Surface area analysis

Surface area analysis by Brunauer–Emmett–Teller method (BET) was used in this study with the objective to compare the surface area and pore volume of RHA calcined at 600 °C and RHA/ Fe_3O_4 composite of various quantities of starting amount of Fe_3O_4 particles (RHA/ Fe_3O_4 10%, RHA/ Fe_3O_4 15% and RHA/ Fe_3O_4 20%). The higher surface area of the adsorbent, the higher adsorption capacity of oil would be obtained [52]. The isotherms are shown in Figure 4.4.

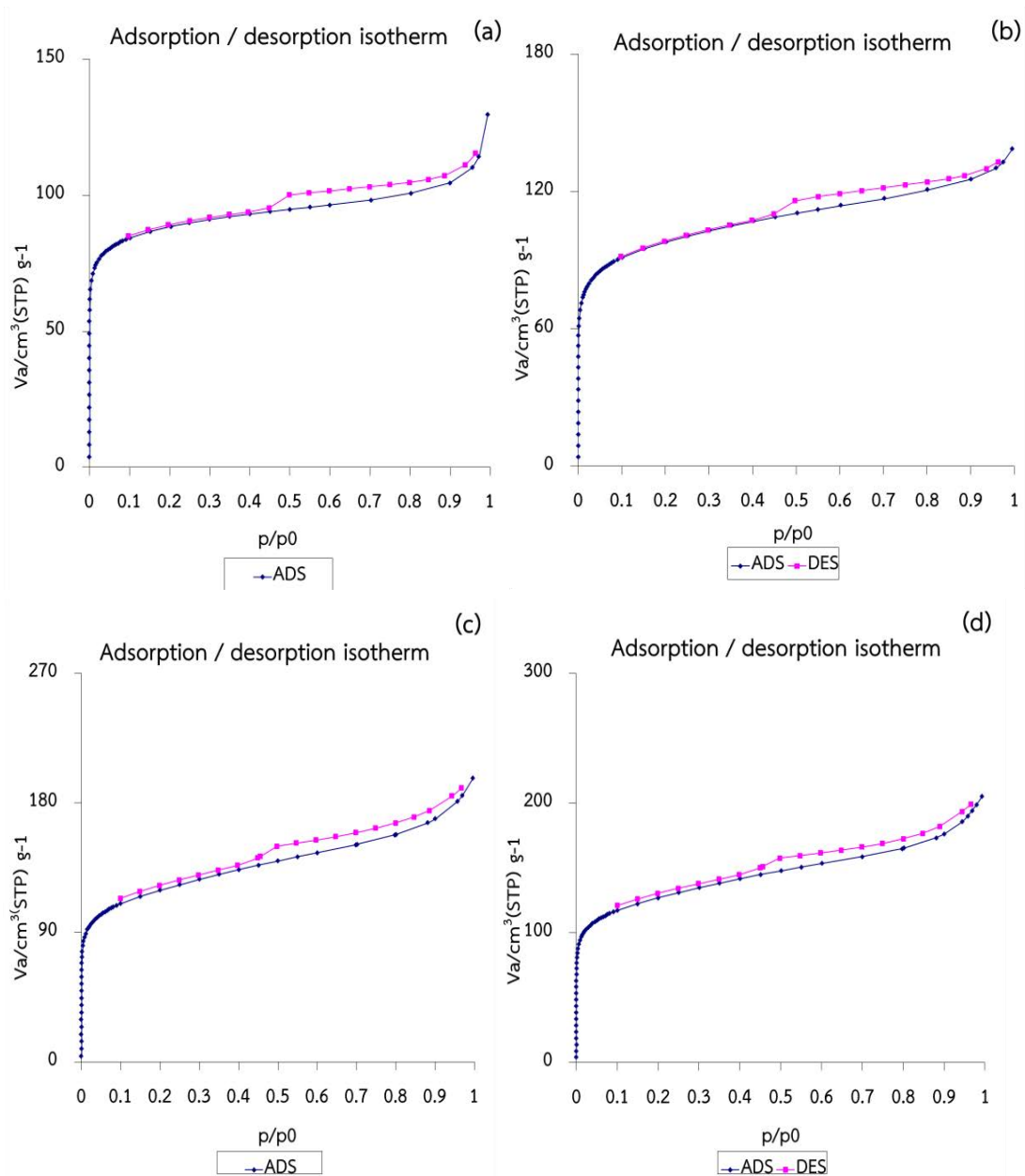


Figure 4.4 Nitrogen adsorption/desorption isotherms of
 (a) RHA size 1-75 μm (b) RHA size 75-150 μm ,
 (c) RHA/ Fe_3O_4 10% size 1-75 μm (d) RHA/ Fe_3O_4 10% size 75-150 μm .

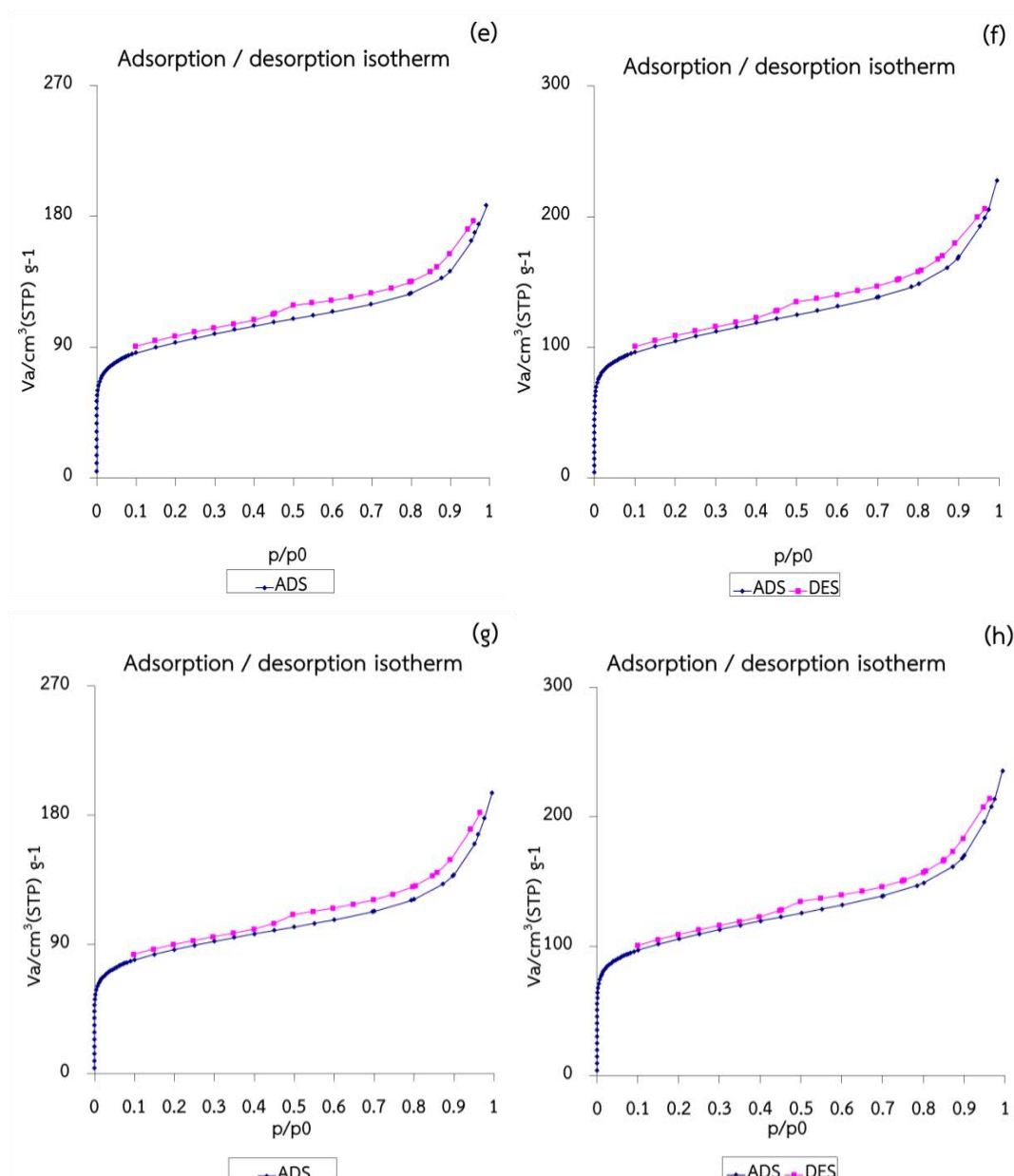


Figure 4.4 Nitrogen adsorption/desorption isotherms of
 (e) RHA/ Fe_3O_4 15% size 1-75 μm (f) RHA/ Fe_3O_4 15% size 75-150 μm
 (g) RHA/ Fe_3O_4 20% size 1-75 μm and (h) RHA/ Fe_3O_4 20% size 75-150 μm .

Regarding the nitrogen adsorption/desorption isotherms of RHA and RHA/ Fe_3O_4 composites, shown in Figure 4.4, a combination of the Type I isotherms indicating the presence of microporous structures according to the IUPAC nomenclature was observed. These sorption isotherms data were used to calculate the specific surface area and total pore volume as shown in Table 4.4.

Table 4.4 Textural characteristics for the RHA and the RHA/Fe₃O₄ composites

Materials	Size of RHA (μm)	Surface area (m^2/g)	Total pore volume (cm^3/g)
RHA@600°C	1-75	386.07	0.1385
RHA@600°C	75-150	443.58	0.1418
RHA/Fe ₃ O ₄ 10%	1-75	491.46	0.1991
RHA/Fe ₃ O ₄ 15%		381.08	0.1312
RHA/Fe ₃ O ₄ 20%		350.94	0.1148
RHA/Fe ₃ O ₄ 10%	75-150	544.53	0.2104
RHA/Fe ₃ O ₄ 15%		438.94	0.1426
RHA/Fe ₃ O ₄ 20%		446.45	0.1393

Table 4.4 presents the specific surface area and total pore volume of the RHA and the RHA/Fe₃O₄ composites. The surface area of RHA calcined at 600 °C, divided into two sizes by sieve analyzer including 1-75 and 75-150 μm , were 386.07, 443.58 m^2/g , respectively. After preparing RHA/Fe₃O₄ composites using 10% of starting Fe₃O₄, the specific surface area of the sorbents increased with the increasing amount of starting Fe₃O₄. But, when adding Fe₃O₄ to 15% and 20%, the specific surface area and total pore volume decreased, due to the presence of Fe₃O₄ on the RHA surface which possibly blocked the pores of RHA. Therefore, RHA/Fe₃O₄10% might lead to have the highest oil adsorption capacity because it has the highest specific surface area.

4.1.5 Thermogravimetric analysis (TGA)

Figure 4.5 (a) shows the TGA curve of RHA@600°C (75-150 μm). The result reveals that the weight loss of RHA@600°C (75-150 μm) is very small (~4%). This suggests that almost carbon in RHA (~36%) is fixed carbon or elemental carbon that is not decomposed under nitrogen atmosphere at the temperature less than 800°C.

From the thermogravimetric weight loss curve of RHA/Fe₃O₄-PS(10% of Fe₃O₄ and 10% of PS, 75-150 μm) composites in Figure 4.5 (b), the initial weight loss in the region of 50-150 °C indicates 2.6 % loss corresponding to the evaporation of

physically adsorbed water. The second weight loss appears at 300–500 °C with 18.4 % loss was found attributing to a carbonization of polystyrene on the material surface and organic constituents of RHA[53] and the weight loss of Fe_3O_4 about ~18% as shown in Figure 4.5 (c) which is in accordance with the literature[54]. The residual weight is considered to be the amount of silica of ash and magnetite of 72% (corresponding to 28% weight loss). By applying the mass balance of weight loss, the approximate total amount of PS in the sample is 10% (equal to 28% (total weight loss) –18% (weight loss of Fe_3O_4)).

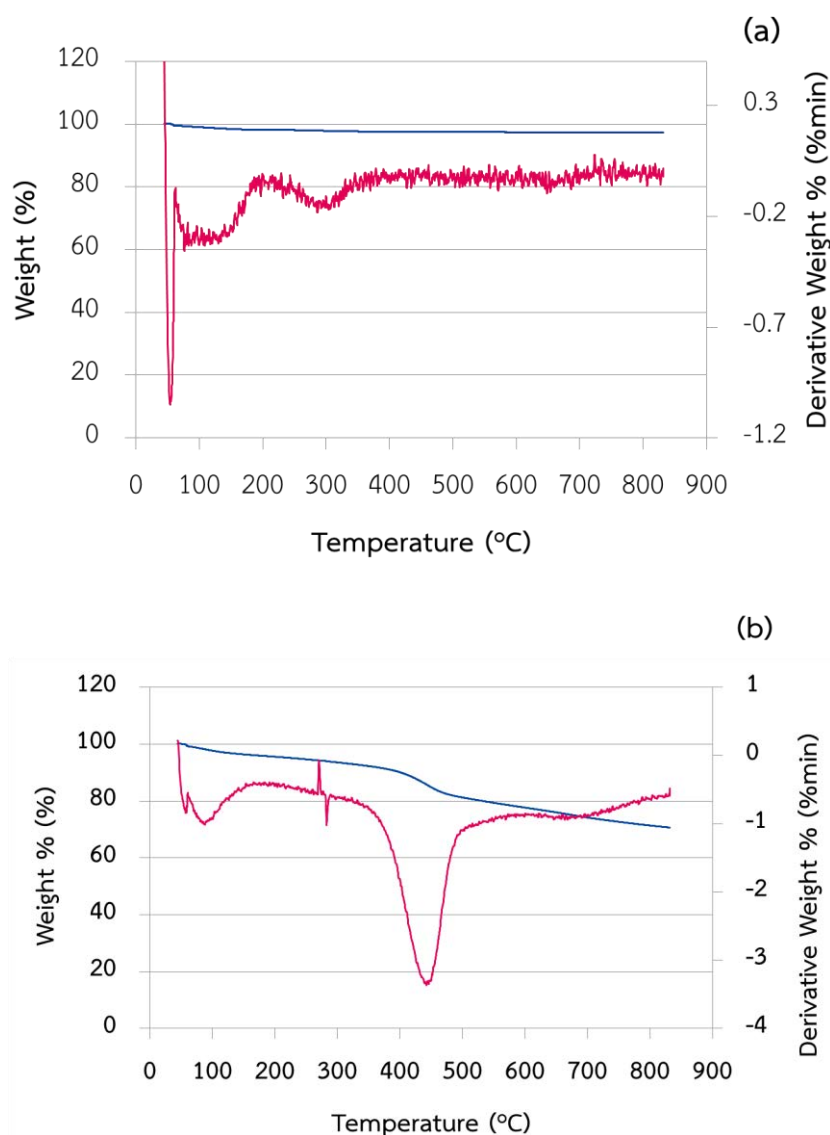


Figure 4.5 Thermogravimetric weight loss curve of (a) RHA@600°C (75-150 μm) and (b) RHA/Fe₃O₄-PS (10% of Fe₃O₄ and 10% of PS, 75-150 μm),

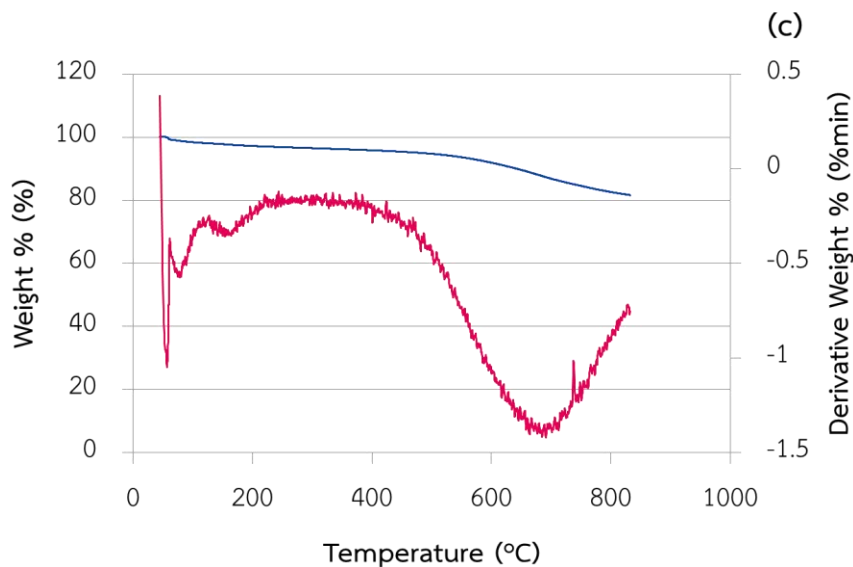


Figure 4.5 Thermogravimetric weight loss curve of (c) Fe_3O_4 .

4.1.6 Contact angles

RHA can be either hydrophilic or hydrophobic. However, when it is calcined at 600°C , it becomes hydrophobic because of high amount of carbon content on the RHA surface. The contact angle (CA) measurement of RHA@ 600°C is depicted in Figures 4.6 (a). It is hydrophobic (CA= 148.3°) because of high amount of carbon. The RHA/ Fe_3O_4 composite became hydrophilic (Figure 4.6(b)). It was possible to obtain a contact angle as the water was immediately adsorbed by the RHA/ Fe_3O_4 because a corollary, low or 0° contact angles of water is associated with hydrophilic properties. The surface of RHA/ Fe_3O_4 composites modified with polystyrene foam became hydrophobic (CA= 136.5°) again, which indicated that water did not adsorb onto the low-energy RHA/ Fe_3O_4 -PS surface.

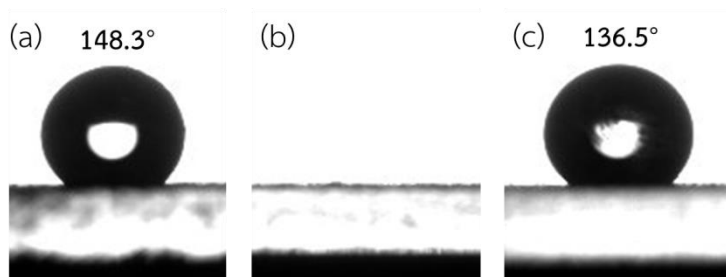


Figure 4.6 Photographs showing a water droplet on the surface of (a) RHA@ 600°C (b) RHA/ Fe_3O_4 , and (c) RHA/ Fe_3O_4 10-PS10.

4.1.7 Fourier transform infrared spectroscopy

RHA, RHA/Fe₃O₄ and RHA/Fe₃O₄-PS were characterized by Fourier transform infrared spectrometry (FTIR) to investigate the presence of specific functional groups on the sample. FTIR spectra of RHA, RHA/Fe₃O₄ and RHA/Fe₃O₄-PS were recorded using potassium bromide (KBr) technique. The characteristic functional groups and the corresponding wavenumbers of RHA and polystyrene are presented in Table 4.5.

Table 4.5 FTIR vibration band position and their assignments for RHA, polystyrene, Fe₃O₄ particles

Adsorbents	Wavenumber (cm ⁻¹)	Remarks and assignment	Ref.
RHA	3750-2800	O-H of silanol and adsorbed water	[55]
	1320	Si-O-Si siloxane bonds	
	1073	Si-O vibrational band	
Polystyrene	3030-3080	Aromatic C-H stretching vibration	[56]
	2000-1650	Aromatic C-H combination frequency overtones	
	1625-1474	Aromatic C-C bonds stretching vibration	
	1250-650	Aromatic C-H deformation vibration	
Fe ₃ O ₄	630-590	Symmetric Fe-O stretching vibration	[57]
	450-400	Antisymmetric Fe-O stretching vibrations	

Figure 4.7 (a) shows the FTIR spectrum of RHA between 400 to 4000 cm^{-1} . The main spectrum composes of large broad band between 3000 to 3700 cm^{-1} which is O-H bond stretching of silanol group on the surface of RHA. The exhibited typical bonds of very strong Si-O-Si stretching are found at 1073 and 798 cm^{-1} and the bands at 476 cm^{-1} correspond to the bending vibrations [55].

Figure 4.7 (b) shows the FTIR spectrum of RHA/ Fe_3O_4 that presents characteristic band of silanol O-H stretching. However, the vibrational absorption peak of $\text{Fe}^{2+}-\text{O}^{2-}$, which should be at 437 cm^{-1} , cannot be detected in the wavenumber range of 500-4000 cm^{-1} .

The FTIR spectrum of RHA/ Fe_3O_4 -PS is illustrated in RHA/ Fe_3O_4 -PS. The presence of polystyrene at 700 cm^{-1} belonged to the flexural vibrations (C-H) of the benzene ring is observed [56]. In addition, distinctively weak characteristic absorption peaks at 1384, 1453 and 1491 cm^{-1} assigned to benzene ring vibrations (C-C) of polystyrene are found [56].

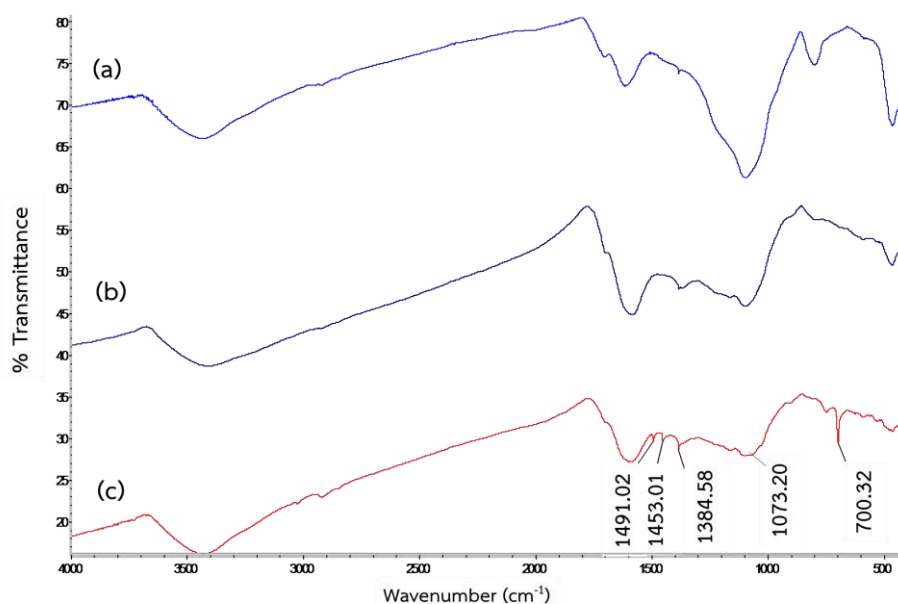


Figure 4.4 FTIR spectrum of (a) RHA@600 °C (b) RHA/10% Fe_3O_4 (c) RHA/ Fe_3O_4 -PS

4.1.8 SEM micrographs and EDX diffractograms

The morphology of RHA/ Fe_3O_4 and RHA/ Fe_3O_4 -PS composite were photographed by scanning electron microscopy as shown in Figure 4.8 and Figure 4.9, respectively. In part of small size composite (1-75 μm), there has a small number of pores due to the fact that the structure of RHA was broken by crushing process. On the other hand, 75-150 μm material has rough surface and wide pore that could enhance the oil sorbent capacity. When the surface of RHA/ Fe_3O_4 was modified by polystyrene,

thin film of polystyrene was observed and the porous structure of RHA/Fe₃O₄ was still unchanged (see Figure 4.9).

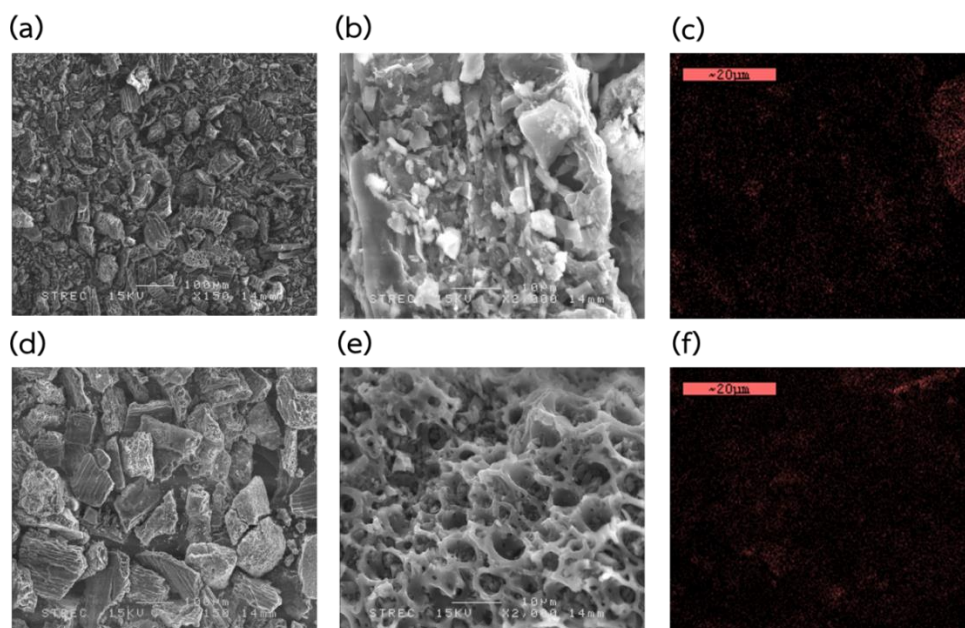


Figure 4.8 The SEM micrographs and EDX elemental mapping of the composites (a) RHA/Fe₃O₄ size 1-75 μm (d) RHA/Fe₃O₄ size 75-150 μm (b,e) Inside the composite matrix and (c, f). Red spots indicate the area where iron signal was detected.

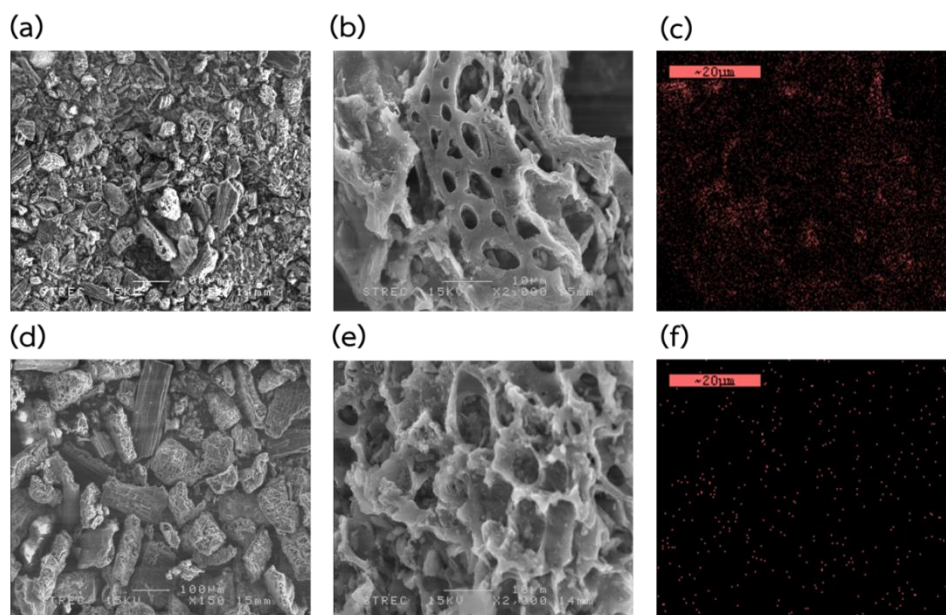


Figure 4.9 The SEM micrographs and EDX elemental mapping of the composites (a) RHA/Fe₃O₄-PS size 1-75 μm (d) RHA/Fe₃O₄-PS size 75-150 μm (b,e) Inside the composite matrix and (c, f). Red spots indicate the area where iron signal was detected.

Figure 4.10 shows the energy dispersive X-ray (EDX) diffractograms of the materials. The elemental micro-analysis of the samples depends on their chemical composition. The result shows that the prepared RHA is highly porous material. The elemental micro-analysis of RHA/Fe₃O₄-PS (Figure 4.10 (b)) indicates a weight percent of C of 88.7%, Si of 9.2%, and Fe of 2.1%. The carbon content in RHA/Fe₃O₄-PS was found to be the highest in Figure 4.10 (b) and higher than that observed in Figure 4.10 (a). It can be assumed that the carbon signal likely comes from polystyrene modified on the surface, while the weight percentage of iron increased when increasing the amount of magnetic particles on RHA.

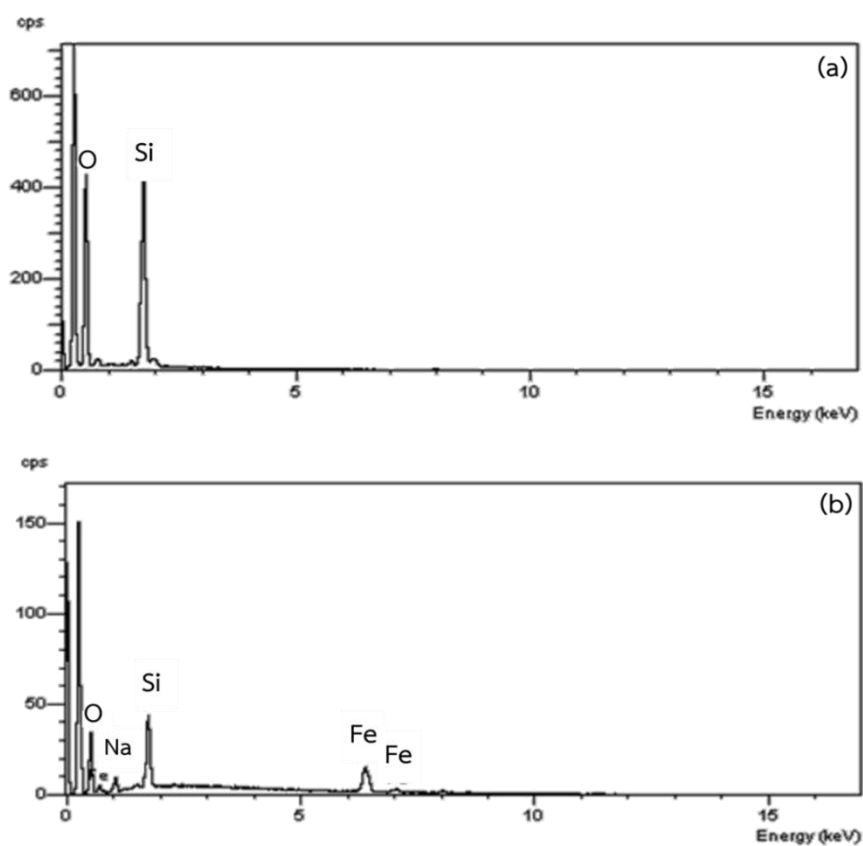


Figure 4.10 EDX diffractogram of (a) RHA@600 °C (b) RHA/Fe₃O₄-PS.

4.2 Adsorption study

Figure 4.11 shows the crude oil adsorption capacity of all composites in this study.

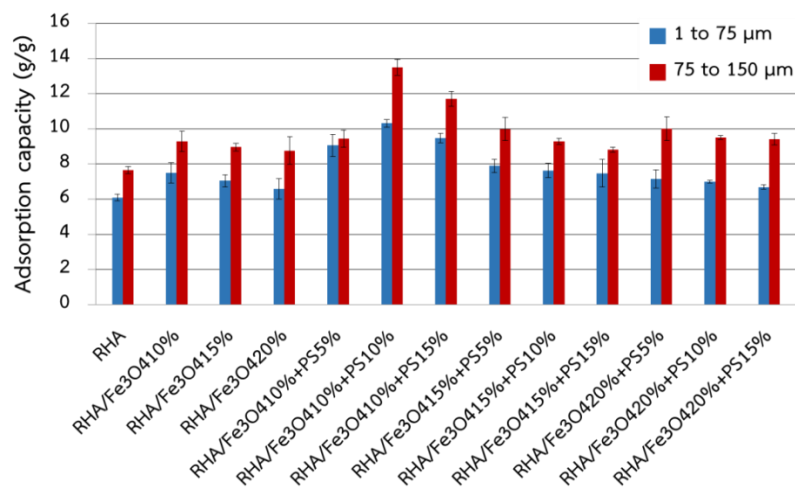


Figure 4.11 Adsorption capacity of the composites.

4.2.1 Effect of RHA size

Table 4.6 shows that the effect of different RHA size was found. Larger particle size sorbent (75-150 μm) can adsorb crude oil more than the smaller one (1-75 μm) because the larger RHA has higher surface area than the smaller particles (see the results in Table 4.4). Furthermore, the difference of oil adsorption capacity depends on the amount of magnetic particles and polystyrene which is demonstrated in Figures 4.12 and 4.13.

Table 4.6 Adsorption capacity of RHA/Fe₃O₄-PS composites

Materials	Adsorption capacity (g/g)	
	Size 1-75 μm	Size 75-150 μm
RHA calcined at 600 °C	6.091±0.196	7.665±0.205
RHA/Fe ₃ O ₄ 10	7.494±0.595	9.287±0.591
RHA/Fe ₃ O ₄ 15	7.041±0.334	8.963±0.224
RHA/Fe ₃ O ₄ 20	6.582±0.574	8.761±0.782
RHA/Fe ₃ O ₄ 10-PS 5	9.052±0.636	9.448±0.485
RHA/Fe ₃ O ₄ 10-PS 10	10.313±0.214	13.505±0.458

Table 4.6 Adsorption capacity of RHA/Fe₃O₄-PS composites

Materials	Adsorption capacity (g/g)	
	Size 1-75 μm	Size 75-150 μm
RHA/Fe ₃ O ₄ 10-PS 15	9.472±0.269	11.702±0.427
RHA/Fe ₃ O ₄ 15-PS 5	7.894±0.379	9.988±0.661
RHA/Fe ₃ O ₄ 15-PS 10	7.630± 0.413	9.281±0.166
RHA/Fe ₃ O ₄ 15-PS 15	7.466±0.784	8.808±0.138
RHA/Fe ₃ O ₄ 20-PS 5	7.148±0.505	10.019±0.676
RHA/Fe ₃ O ₄ 20-PS 10	6.984± 0.086	9.511±0.110
RHA/Fe ₃ O ₄ 20-PS 15	6.685±0.123	9.412±0.316

4.2.2 Effect of Fe₃O₄ loading

The adsorption capacity of RHA/Fe₃O₄ composites with different amount of starting Fe₃O₄ is showed in Figure 4.12. The oil adsorption capacity of RHA/Fe₃O₄ was higher than that of unmodified RHA due to higher specific surface area. However, the adsorption capacity of RHA/Fe₃O₄ composites with different amount of starting Fe₃O₄ was quasi-similar. This could be explained that the content of magnetic particles in the material determined by FAAS (see Table 4.3) was not significantly different. The adsorption capacity of the larger particles (75-150 μm) was higher than the smaller ones (1-75 μm) owing to higher specific surface area.

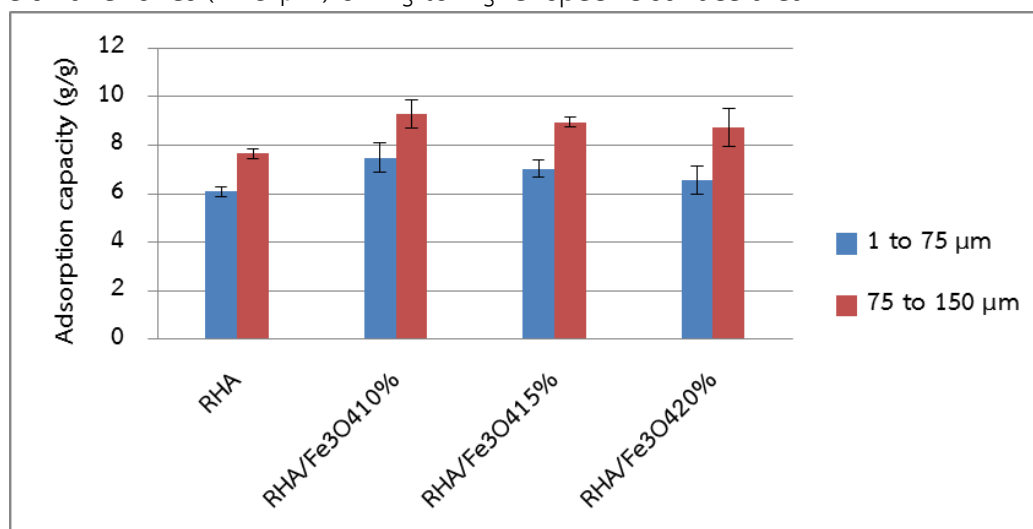


Figure 4.12 Adsorption capacity of RHA/Fe₃O₄ composites prepared by using different amount of Fe₃O₄.

4.2.3 Effect of polystyrene loading

RHA/Fe₃O₄-PS sorbents prepared by using different amounts of polystyrene in a range of 5 to 15 %w/w were subject to investigate crude oil adsorption capacity.

The adsorption capacity of RHA/Fe₃O₄-PS is shown in Figure 4.13. It was found that RHA/Fe₃O₄-PS could adsorb oil with high adsorption capacity (12.522 g/g) than RHA/Fe₃O₄. When increasing the amount of polystyrene, the oil adsorption capacity increased. However, at higher amount of polystyrene (15%), the adsorption capacity decreased slightly. This might be due to the fact that polystyrene could block or cover the pores of RHA adsorbent, thus oil adsorption capacity decreased.

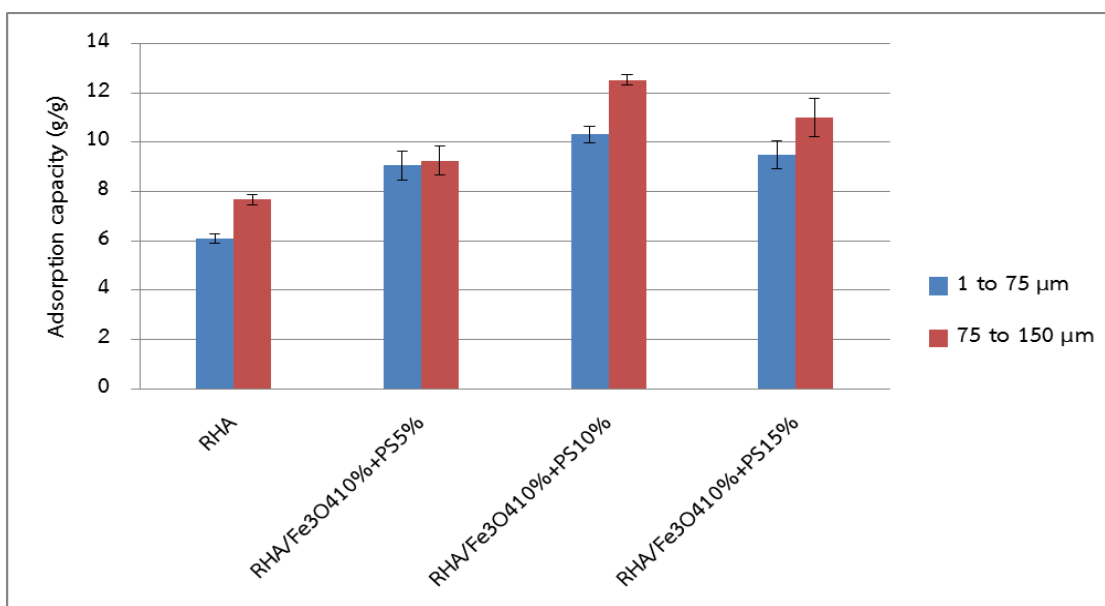


Figure 4.13 Adsorption capacity of RHA/Fe₃O₄-PS composites prepared by using different amounts of polystyrene.

4.2.4 Effect of contact time

Figure 4.14 shows that within only 10 minutes, RHA/Fe₃O₄-PS could remove oil with high adsorption capacity (5.937 g/g). Eventhough, when increasing of contact time, the amount of oil adsorbed increased and reached the equilibrium (12.522 g/g) after 40 minutes.

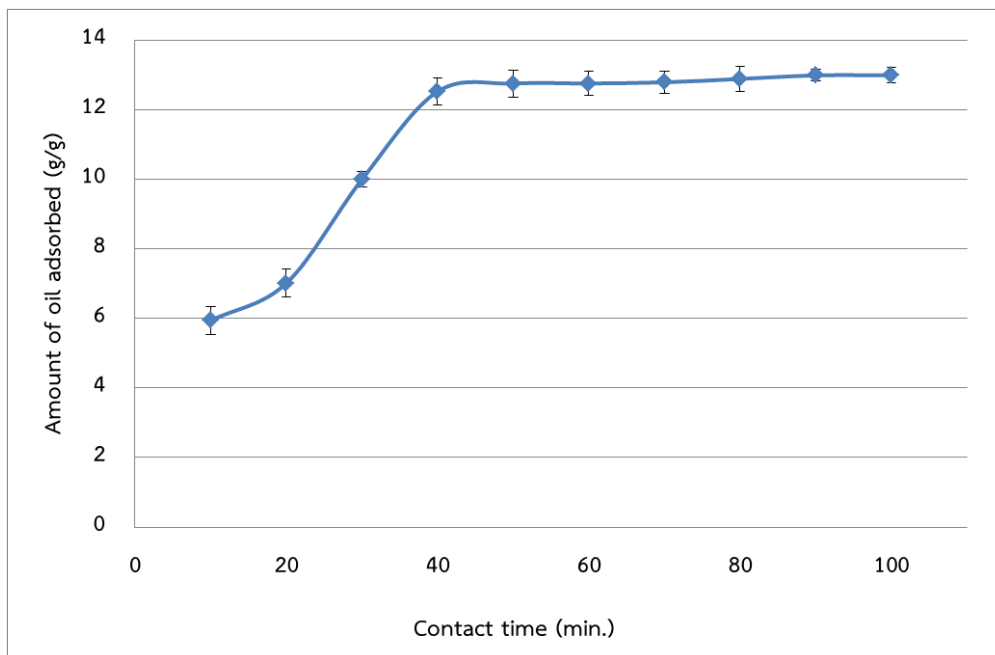


Figure 4.14 Effect of adsorption time on oil adsorption of RHA/Fe₃O₄-PS

When compared the oil adsorption capacity of RHA/Fe₃O₄-PS to other adsorbents reported by other authors (Table 4.7), the adsorbent prepared in this study showed a good oil adsorption capacity (12.522 g/g) and also has magnetic property that could be easily separated from a contaminated area after adsorption.

Table 4.7 The maximum adsorption capacity of the RHA/Fe₃O₄-PS compared to other modified silica for oil adsorption.

Adsorbent	Pyrolyzed Temp (°C)	Oil type	Adsorption capacity (g/g)	Ref.
White rice husk ash	800	Diesel fuel	2.78	[5]
		Crude oil	2.98	
Black rice husk ash	500	Diesel fuel	5.02	[5]
		Crude oil	6.22	

Table 4.7 The maximum adsorption capacity of the RHA/Fe₃O₄-PS compared to other modified silica for oil adsorption.

Adsorbent	Pyrolyzed Temp (°C)	Oil type	Adsorption capacity (g/g)	Ref.
Rice husk ash	600–700	Heavy crude oil	6	[46]
Rice husk ash	250	Crude oil	9	[47]
	350		9.2	
	480		9.4	
	700		8.8	
Rice husk ash	480	Gasoline	3.7	[48]
		Diesel	5.5	
		Light crude oil	6.0	
		Motor oil	7.5	
		Heavy crude oil	9.2	
Silica aerogel		Vegetable oil	14.6	[58]
		Motor oil	15.1	
		Crude oil	11.7	
RHA/Fe ₃ O ₄ -PS(10%)	600	Crude oil	12.522	This work

4.3 Separation of the composites from water/oil mixture by a permanent magnet

Figure 4.15 presents the demonstration of the adsorbent separated by external magnetic field. It was observed that the composites were very good buoyancy and could adsorb crude oil on the surface of the water/crude oil mixture. The composites were agglomerated when applied an external magnetic field and adsorbent possessing crude oil could be removed from the contaminated area.

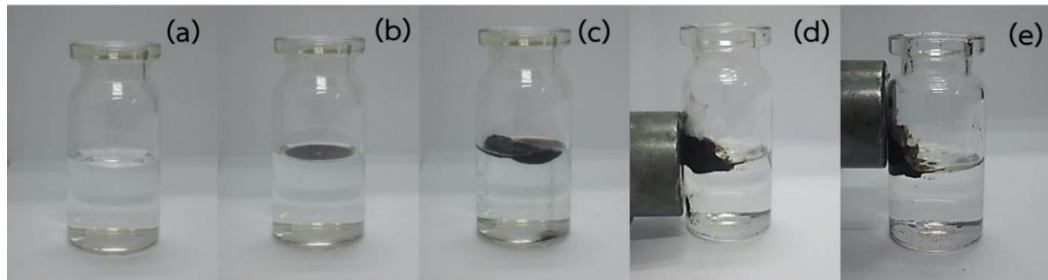


Figure 4.15 The demonstration of used adsorbent separation by an external magnetic field: (a) Pure water (b) Water/crude oil mixture (c) the process of crude oil sorption by the prepared adsorbent (d) magnetic separation of the adsorbent (e) removal of the adsorbent from the surface of water.

CHAPTER V

CONCLUSION

5.1 Conclusion

Rice husk ash–magnetic particles surface-modified with polystyrene (RHA/Fe₃O₄-PS) was synthesized. The prepared composites were used for crude oil adsorption. The separation and removal process of the adsorbents after being used from water surface was successful by applying an external magnetic field. The composites of RHA and magnetic particles were prepared using co-precipitation of ferric iron (Fe³⁺), ferrous iron (Fe²⁺) and RHA using various quantities of starting Fe₃O₄ particles ranging from 10-20 g of Fe₃O₄ per 100 g of RHA (0.4185-0.7640 mmol/g composite). The amount of added Fe₃O₄ of 0.4185 mmol/g composite allowed the deposition of Fe₃O₄ on RHA of 0.1143 mmol/g composite and it is enough to make the composites respond to an external magnetic field. The adsorbents of 10% of starting Fe₃O₄ had the highest surface area. In this work, RHA/Fe₃O₄ composites could be applied as sorbents for eliminating oil spill. Since the surface of RHA/Fe₃O₄ composite have hydrophilic properties that could affect the oil adsorption ability because of the non-polarity of oil, the hydrophobicity of RHA/Fe₃O₄ surface was thus improved by coating with polystyrene (PS). RHA/Fe₃O₄ composites were then modified with waste polystyrene foam of various weight percentages ranging from 5–20% of RHA/Fe₃O₄. The effect of polystyrene on the adsorption capacity was found that RHA/Fe₃O₄-PS (10% of starting Fe₃O₄ and 10% of PS) could adsorb oil with the highest adsorption capacity (12.522 g/g). When using higher amount of polystyrene (15%), the adsorption capacity decreased. Finally, when compare the oil adsorption capacity of RHA/Fe₃O₄-PS to other adsorbents reported by other authors, the RHA/Fe₃O₄-PS prepared in this study showed a good oil adsorption capacity (12.522 g/g) and also has a magnetic property. The adsorbent could be easily separated from a contaminated area after adsorption due to its magnetic property.

5.2 Suggestions

- The sorption capacity should be studied on more various types of oil such as vegetable oil, motor oils, gasoline, and diesel oils.
- Other types of synthetic polymer such as polyester, polyurethane, polyacrylamide as well as natural polymers such as chitosan and cellulose shall be used for the surface modification of RHA/Fe₃O₄.
- A pilot study of the adsorption process shall be investigated in larger scale.

REFERENCES

- [1] Liou, T.H., *Evolution of chemistry and morphology during the carbonization and combustion of rice husk*. Carbon, 2004. **42**(4): p. 785-794.
- [2] Richard, B., *Biotechnology of petroleum pollutant biodegradation*. Microbial Ecology, 1986. **12**: p. 155-172.
- [3] Al-Sabagh, A.M.,Nehal, S.A., Amal, M.N. and Gabr, M.M., *Synthesis and evaluation of some polymeric surfactants for treating crude oil emulsions*. Colloids and Surfaces A: Physicochemical and Engineering Aspects, 2003. **216**(1-3): p. 9-19.
- [4] Charusheela, A. and Modi, H.A., *Study of bacterial diversity of crude oil degrading bacteria isolated from crude oil contaminated sites*. Life sciences Leaflets 2012. **6**: p. 13-23.
- [5] Vlaev, L.,Petkov, P., Dimitrov, A. and Genieva, S., *Cleanup of water polluted with crude oil or diesel fuel using rice husks ash*. Taiwan Institute of Chemical Engineers, 2011. **42**(6): p. 957-964.
- [6] Carmody, O., Frost, R. and Kokot, S., *Adsorption of hydrocarbons on organo-clays-implications for oil spill remediation*. Colloid Interface Science, 2007. **305**(1): p. 17-24.
- [7] Bastani, D., Safekordi,A.A., Alihosseini,A. and Taghikhani, V., *Study of oil sorption by expanded perlite at 298.15K*. Separation and Purification Technology, 2006. **52**(2): p. 295-300.
- [8] Li, H., Liu, L. and Yang,F., *Oleophilic polyurethane foams for oil spill cleanup*. Procedia Environmental Sciences, 2013. **18**: p. 528-533.
- [9] Suni, S.,Kosunen,A., Hautala,M., Pasila,A. and Romantschuk, M., *Use of a by-product of peat excavation, cotton grass fibre, as a sorbent for oil-spills*. Marine Pollution Bulletin, 2004. **49**(11-12): p. 916-21.
- [10] Foo, K.Y. and Hameed, B.H., *Utilization of rice husk ash as novel adsorbent: A judicious recycling of the colloidal agricultural waste*. Advances in Colloid and Interface Science, 2009. **152**(1-2): p. 39-47.
- [11] Jones, J.D., *A new refractory from vegetable source*. Canadian Metals, 1953. **16**: p. 22-24.
- [12] Yalcin, N. and Sevinc, V., *Studied on silica obtained from rice husk*. Ceramics International 2001. **27**: p. 219-224.
- [13] Prasad, R. and Pandey, M., *Rice husk ash as a renewable source for the production of value added silica gel and its*. Bulletin of Chemical Reaction Engineering & Catalysis, 2012. **7**: p. 1-25.

- [14] Fungsin, B., *Utilization of cellulose to facilitate isolation silica from rice husk*, 1995, Master's Thesis. Department of Microbiology Science, Graduate School, Chulalongkorn University.
- [15] Tarateerapap, T., *Metal extraction from aqueous solution using Schiff's base functionalized mesoporous silica*, 2004, Master's Thesis. Department of Environmental Science, Graduate School, Chulalongkorn University.
- [16] Patel, M., Karera, A. and Prasanna, P., *Effect of thermal and chemical treatments on carbon and silica contents in rice husk*. Materials Science., 1987. **22**: p. 2457-2464.
- [17] Ramli, Z., *Rhenium-impregnated zeolites: synthesis, characterization and modification as catalysts in the metathesis of alkanes*, 1995, Teknologi Malaysia.
- [18] Breck, D.W., *Zeolite Molecular Sieves*. 1974, London, UK: John Wiley & Sons.
- [19] Seiichiro, T., Horonori, I., Takeshi, H. and Shinichiro, Y., *Hierarchical porous carbon from cell assemblies of rice husk for in vivo applications*. Medicinal Chemistry Communications, 2010. **1**: p. 136-138.
- [20] Ozgur, U., Alivov, Y. and Morkoc, H., *Microwave ferrites, part 1: fundamental properties*. Materials Science: Materials in Electronics, 2009. **20**: p. 789-834.
- [21] Chikazumi, S., *Physics of Magnet* 1964, New York, USA: John Wiley & Sons.
- [22] Gareth, S.P., Novotný, Z., Peter, J., Michael, S. and Diebold, U., *A metastable Fe(A) termination at the Fe₃O₄(001) surface*. Surface Science 2011. **605**: p. L42-L45.
- [23] Mehta, S., Biederman, S. and Shivkumar, S., *Thermal degradation of foamed polystyrene*. Materials Science, 1995: **30**: p. 2944-2949.
- [24] Islam, M.R., Chhetri, A.B. and Khan, M.M., *The greening of petroleum operations*. The Science of Sustainable Energy Production. 2010, Salem, USA: Scrivener Publishing John Wiley & Sons.
- [25] Sun, X.L., Fan, Z.P., Zhang, L.D., Wang, L., Wei, Z.J., Wang, X.Q. and Liu, W.L., *Superhydrophobicity of silica nanoparticles modified with polystyrene*. Applied Surface Science 2011. **257**: p. 2308-2312.
- [26] Lin, J., Shang, Y., Ding, B., Yang, J., Yu, J. and Al-Deyab, S.S., *Nanoporous polystyrene fibers for oil spill cleanup process used as oil sorbents for oil spill cleanup*. Marine Pollution Bulletin 2012. **64** p. 347-352.
- [27] *Chemicals in the environment: 1,2,4-trimethylbenzene*. 1994 [cited 2012 September 2]; The Agency for Toxic Substances and Disease Registry]. Available from: http://www.epa.gov/chemfact/f_trimet.txt.

- [28] Ellis, B., Balba, M.T. and Theile, P., *Bioremediation of oil contaminated land*. Environmental Technology, 1990. **11**: p. 443-454.
- [29] Duffy, J.J., Peake, E. and Mohtadi, M.F., *Oil spills on land as potential sources of groundwater contamination*. Environment International, 1980. **3**: p. 107-120.
- [30] Kim, H., Hong, S.H., Won, J., Yim, U.H., Jung, J.H., Ha, S.Y., Kim, E., Han, G.M., Baek, S., Choi, H.W. and Shim, W.J., *Petroleum hydrocarbon contaminations in the intertidal seawater after the Hebei Spirit oil spill effect of tidal cycle on the TPH concentrations and the chromatographic characterization of seawater extracts*. Water Research 2013. **47**: p. 758-768.
- [31] Atle, B.N., James, L.S. and Kenneth, R.B., *Oil and water separation in marine oil spill clean-up operations spill*. Science and Technology Bulletin, 1996. **3**: p. 107-122.
- [32] Muttin, F., *Structural analysis of oil spill containment booms in coastal and estuary waters*. Applied Ocean Research, 2008. **30**(2): p. 107-112.
- [33] Broje, V. and Keller, A.A., *Effect of operational parameters on the recovery rate of an oleophilic drum skimmer*. Hazardous Materials, 2007. **148**: p. 136-143.
- [34] Atlas, R.M. and Cerniglia, C.E., *Bioremediation of petroleum pollutants*. Bioscience, 1995. **45**: p. 332-339.
- [35] Lewis, A., Ken, T.B., Randy, C.B. and Joseph, V.M., *Large scale dispersant leaching and effectiveness experiments with oils on calm water*. Marine Pollution Bulletin, 2010. **60**: p. 244-254.
- [36] Abdul, A.A., Abdulrauf, R.A. and Hossain, M.E., *A sustainable approach to controlling oil spills*. Environmental Management 2012. **113**: p. 213-227.
- [37] Ladd, R.W. and Smith, D.D., *System study of oil spill cleanup procedure*. Society of Petroleum Engineers, 1970. **30**: p. 1-30.
- [38] McLeod, W.R. and McLeod, D.L., *Measures to combat arctic and subarctic oil spills*. Petroleum Engineers, 1974. **25**: p. 1-10.
- [39] Masomeh, S.M., Saeed, B., Morteza, T. and Ali, N., *Adsorption of petroleum hydrocarbons on organoclay*. Applied Chemical Researches, 2010. **4**: p. 19-23
- [40] Sokkera, H.H., Naeem, M.E., Hassanc, M.A. and Bahgat, E.E., *Adsorption of crude oil from aqueous solution by hydrogel of chitosan based polyacrylamide prepared by radiation induced graft polymerization*. Hazardous Materials, 2011. **190**: p. 359-365.

- [41] Singh, R. and Dhindaw, B.K., *Production of high purity silicon for use in solar cells*. Proceedings of the International Solar Energy Congress, 1978. **35**: p. 776-781.
- [42] Kim, K.D. and Sung, S.K., *Formation and characterization of silica-coated magnetic nanoparticles by sol-gel method*. Industrial and Engineering Chemistry, 2005. **11**: p. 584-589.
- [43] Dong, L., Yi, L., Jianping, D. and Wantai, Y., *Synthesis and characterization of magnetic Fe_3O_4 -silica-poly(γ -benzyl-L-glutamate) composite microspheres*. Reactive and Functional Polymers, 2011. **71**(10): p. 1040-1044.
- [44] Nwankwere, E.T., Gimba, C.E., Kagbu, J.A. and Nale, B.Y., *Sorption studies of crude oil on acetylated rice husks*. Applied Science Research, 2010. **2**: p. 142-151.
- [45] Seiji, K., Yosuke, N., Yasuji, K. and Koichi, T., *Oil adsorbent produced by the carbonization of rice husks*. Waste Management, 2007. **27**: p. 554-561.
- [46] Uzunov, I., *Effects of the pyrolysis process on the oil sorption capacity of rice husk*. Journal of Analytical and Applied Pyrolysis, 2012. **98**: p. 166-176.
- [47] Kenes, K., *Study on the effectiveness of thermally treated rice husks for petroleum adsorption*. Journal of Non-Crystalline Solids, 2012. **358**(22): p. 2964-2969.
- [48] Wypych, G., *Handbook of Solvents* 2001: ChemTec Publishing.
- [49] Kalderis, D., Bethanis, S., Paraskeva, P., and Diamadopoulos, E., *Production of activated carbon from bagasse and rice husk by a single-stage chemical activation method at low retention time*. Bioresource Technology, 2008. **99**: p. 6809-6816.
- [50] Chen, X.G., Shuang, S., Zhang, P.P., Zhang, L., and Ying, Y., *Thermal destruction of rice hull in air and nitrogen*. Thermal Analysis and Calorimetry, 2011. **104**: p. 1055-1062.
- [51] Verónica, R., Elías, M., Oliva, I., Eliana, G., Vaschetto, S., Urreta, E., Griselda, A. and Eimer, S.P., *Silvetti magnetic properties of iron loaded MCM-48 molecular sieves*. Magnetism and Magnetic Materials, 2010. **322**: p. 3438-3442.
- [52] Chandrasekhar, S., Pramada, P.N. and Majeed, J., *Effect of calcination temperature and heating rate on the optical properties and reactivity of rice husk ash*. Materials Science, 2006. **41**: p. 7926-7933.
- [53] Jeongwoo, L., Hong, C.K., Choe, S.S. and Sang, E., *Synthesis of polystyrene/silica composite particles by soap-free emulsion*

polymerization using positively charged colloidal silica. Colloid and Interface Science 2007. **310**: p. 112-120.

- [54] Monica, S., Tianhong, X., Adam, W., Marina, D.M. and Michael, E.M., *Studies on structural, magnetic and thermal properties of $x\text{Fe}_2\text{TiO}_4(1-x)\text{Fe}_3\text{O}_4(0 \leq x \leq 1)$ pseudo-binary system*. Magnetism and Magnetic Materials, 2012. **324**: p. 1453–1462.
- [55] Kalapathy, U., Proctor, A. and Shultz, J., *A simple method for production of pure silica from rice hull ash*. Bioresource Technology 2000. **73**: p. 257-262.
- [56] Muhammed, M.R., Wee, T.T., Mohamad, Z.B. and Anuar, B.K., *Synthesis and characterization of grafted acrylonitrile on polystyrene modified with activated carbon using gamma-irradiation*. Scientific Research and Essays, 2012. **7(7)**: p. 790-795.
- [57] Predoi, D., *A study on iron oxide nanoparticles coated with dextrin obtained by coprecipitation*. Nanomaterials and Biostructures, 2007. **2**: p. 169-173.
- [58] Wang, D., McLaughlin, E., Pfeffer, R. and Lin, Y.S., *Adsorption of oils from pure liquid and oil-water emulsion on hydrophobic silica aerogels*. Separation and Purification Technology, 2012. **99**: p. 28-35.

VITA

Miss Natthaporn Warreewat was born on September 16, 1988 in Saraburi, Thailand. She graduated with a Bachelor degree of Environmental Science from Chulalongkorn University in 2010. After that, she has been a graduated student at the Program in Petrochemistry and Polymer Science, Chulalongkorn University and become a member of Environmental Analysis Research Unit. In 21-23 October 2013, she attended the Science and Technology of Thailand Conference in the title of “Composites of rice husk ash- magnetic particle-polystyrene as oil sorbents” by poster presentation. She finished her Master's degree of Science in 2013.